AFRL-HE-BR-TR-1998-0039

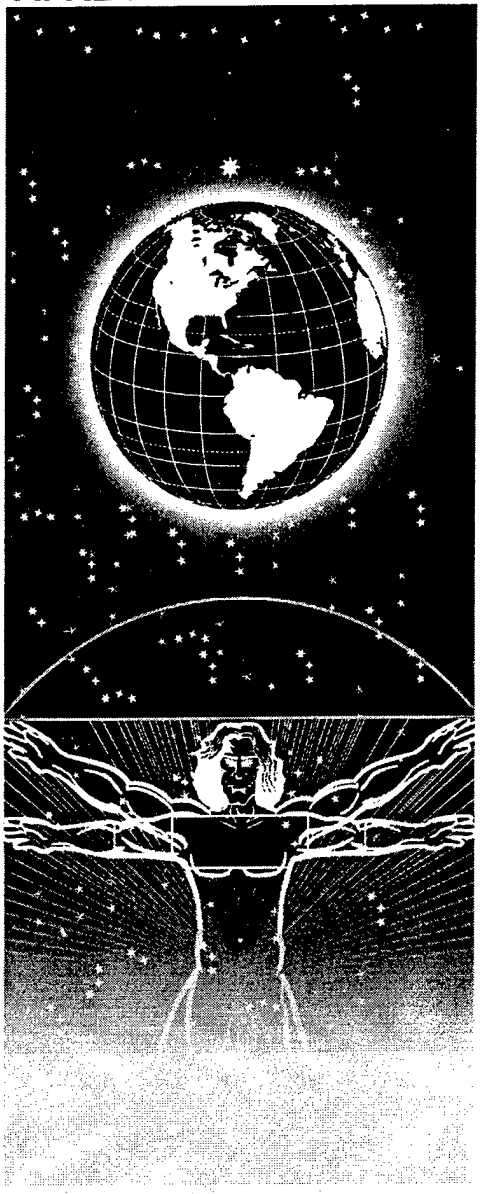

UNITED STATES AIR FORCE RESEARCH LABORATORY

A COMPUTER MODEL FOR LUNG PRESSURE TRANSIENT PREDICTION

John Bomar

BIODYNAMICS RESEARCH CORPORATION
9910 IH 10 West, Suite 1000
San Antonio TX 78230

HUMAN EFFECTIVENESS DIRECTORATE
FLIGHT STRESS PROTECTION DIVISION
SYSTEMS RESEARCH BRANCH
2504 Gillingham Drive, Ste 25
Brooks Air Force Base TX 78235-5104

May 1998

Approved for public release; distribution is unlimited.

NOTICES

When Government drawings, specifications, or other data are used for any purpose other than in connection with a definitely Government-related procurement, the United States Government incurs no responsibility or any obligation whatsoever. The fact that the Government may have formulated or in any way supplied the said drawings, specifications, or other data, is not to be regarded by implication, or otherwise in any manner construed, as licensing the holder, or any other person or corporation; or as conveying any rights or permission to manufacture, use, or sell any patented invention that may in any way be related thereto.

The Office of Public Affairs has reviewed this technical report, and it is releasable to the National Technical Information Service, where it will be available to the general public, including foreign nationals.

This technical report has been reviewed and is approved for publication.

Donald A. Diesel

DONALD A. DIESEL, Maj, USAF, BSC
Project Scientist

Roger L. Stork

ROGER L. STORK, Col, USAF, BSC
Chief, Flight Stress Protection Division

REPORT DOCUMENTATION PAGE

Form Approved
OMB No. 0704-0188

1. AGENCY USE ONLY (Leave blank)	2. REPORT DATE	3. REPORT TYPE AND DATES COVERED
	May 1998	Sep 1993 – Dec 1995

4. TITLE AND SUBTITLE

A Computer Model for Lung Pressure Transient Prediction

5. FUNDING NUMBERS

C – F41624-94-D-4001
PE – 62202F
PR – 7184
TA – 58
WU – 01

6. AUTHOR(S)

John Bomar

7. PERFORMING ORGANIZATION NAME(S) AND ADDRESS(ES)

Biodynamics Research Corporation
9910 IH 10 West, Suite 1000
San Antonio TX 78230

8. PERFORMING ORGANIZATION REPORT NUMBER

9. SPONSORING/MONITORING AGENCY NAME(S) AND ADDRESS(ES)

Air Force Research Laboratory
Human Effectiveness Directorate
Flight Stress Protection Division
Systems Research Branch
2504 Gillingham Drive, Ste. 25
Brooks AFB TX 78235-5104

10. SPONSORING/MONITORING AGENCY REPORT NUMBER

AFRL-HE-BR-1998-0039

11. SUPPLEMENTARY NOTES

12a. DISTRIBUTION/AVAILABILITY STATEMENT

Approved for public release; distribution is unlimited.

12b. DISTRIBUTION CODE

13. ABSTRACT (Maximum 200 words)

The Lung Pressure Transient (LPT) Model demonstrated that computer modeling can be used as a powerful adjunct to Man-Rating testing. A previously developed Aviator's Breathing System (ABS) used to model dynamic response of the human breathing system during rapid decompression (RD) was updated to include simple mechanical models of the lung, diaphragm, and chest wall. The resulting model known as the LPT Model was created to aid estimation of the time histories of differential pressures and transient lung expansion resulting from rapid decompression. The Air Force requested that the implementation of the LPT Model be tailored to model the Aircrew Eye-Respiratory Protective (AERP) System. The LPT Model's predicition agreed fairly closely with the unmanned experimental RDs conducted at the Air Force Research Laboratory, Human Effectiveness Directorate, Flight Stress Protection Division. Using this model, the lung expansions predicted for the MBU-19/P AERP Ensemble were higher than those predicted in simulations without added breathing resistance. However, lung expansions did not seem to be unduly high even when mask and lung peak pressures were high. The authors felt this was encouraging, but the dynamic response of the lung model still needs to be validated to determine if predicting the RDs using the LPT model is safe.

14. SUBJECT TERMS

Aviator's Breathing System (ABS)
Computer modeling;
Lung Pressure Transient (LPT) Model

15. NUMBER OF PAGES

68

16. PRICE CODE

17. SECURITY CLASSIFICATION OF REPORT	18. SECURITY CLASSIFICATION OF THIS PAGE	19. SECURITY CLASSIFICATION OF ABSTRACT	20. LIMITATION OF ABSTRACT
Unclassified	Unclassified	Unclassified	UL

CONTENTS

FIGURES

Figure No.

FIGURES (Continued)

A COMPUTER MODEL FOR LUNG PRESSURE TRANSIENT PREDICTION

1.0 Organization of the Final Report. This final report is organized into five sections. This section, Section 1, presents an overview of the project and BRC's recommendations. Section 2, presents the details of the mathematical model and its theory, while Section 3 presents the results of the simulations conducted with the model. Section 4 is a collection of miscellaneous documents related to establishing the model parameters necessary to characterize the model components. Finally, Section 5 contains a partial source listing of the computer model.

1.1 Introduction and Overview. USAF breathing regulators are equipped with outlet relief valves designed to limit the rise in differential mask pressures to levels that are well tolerated by adults. With older breathing systems, relief valves were usually spring loaded to hold pressures slightly above the required breathing pressure at 47,000 ft altitude. Simple "pop-off valves" limited regulator outlet pressures to approximately 45-52 mmHg (6-7 kPa). In contrast, modern regulators which support pressure breathing for G (PBG) and high altitude pressure breathing (PBA) are required to produce mean breathing pressures as high as 70-75 mmHg (9.3-10 kPa) while simultaneously providing protective relief via compensated relief valves.

Sudden loss of cabin pressurization can lead to a transient rise in transthoracic differential pressure together with high transmural pressures in the lungs. If the loss of pressure is catastrophic, the fall in cabin pressure is so rapid that there is insufficient time for the pressure in the lungs to equilibrate with the external pressure. In such cases it is possible to develop transthoracic pressures approaching the original cabin differential pressure, which, in turn, can produce life threatening pneumothorax and air emboli in exposed aircrew. Any resistance added to the expiratory path by aircrew breathing equipment further impedes the flow of gases from the lung and exacerbates the problem.

It is generally accepted that static transpulmonary pressures over 80-100 mmHg (10.6-13.3 kPa) are unsafe for the relaxed chest.[1] Some tolerance for transient pressure rise is generally allowed, but there are presently no good methods for selecting the allowable peak pressure or its duration. Ernsting[2] has reported evidence that peak pressures up to 100 mmHg are acceptable for periods of less than 50 ms, but no reference for the datum was given.

Further research is needed to define human tolerance to transient transpulmonary pressures. The work described below was aimed at developing a theoretical computer model, which can be employed as a tool to predict the time history of transient pressures within the aviator's breathing system under various rapid decompression scenarios.

1.2 Methods. In 1994 BRC completed SBIR Phase I work in which a preliminary model of the Aviator's Breathing System (ABS) was developed.[3] For the present study, the basic ideas, developed for the ABS model, were extended to add a model of the dynamic response of the breathing system to rapid decompression (RD). In addition, simple mechanical models of the lung, diaphragm, and chest wall were added. The resulting model known as the Lung Pressure Transient (LPT) Model was created to aid estimation of the time histories of differential

pressures and transient lung expansion resulting from rapid decompression. The mechanical response of the thorax was modeled using lumped mechanical properties according to a model originally proposed by Mead and Milic-Emili[4].

The Air Force requested that the first implementation of the LPT Model, be tailored to model the Aircrew Eye-Respiratory Protective (AERP) System. This system comprises the standard USAF Diluter-Demand breathing regulator, CRU-73, a 36-inch regulator outlet hose, and the aircrew headgear, the MBU-19/P. Figure 1.2-1 is a drawing of the MBU-19/P system supplied by its manufacturer, Gentex Corporation. During normal breathing, gas enters the system through the short hose connected to the NBC canister, passes through the NBC canister and mask tube into the oronasal mask via the inspiratory valve. On expiration, gas passes through the shrouded expiratory valve into the environment. A schematic drawing of the AERP system, which was modeled, is shown in Figure 1.2-2.

Figure 1.2-1: MBU-19/P AERP Ensemble

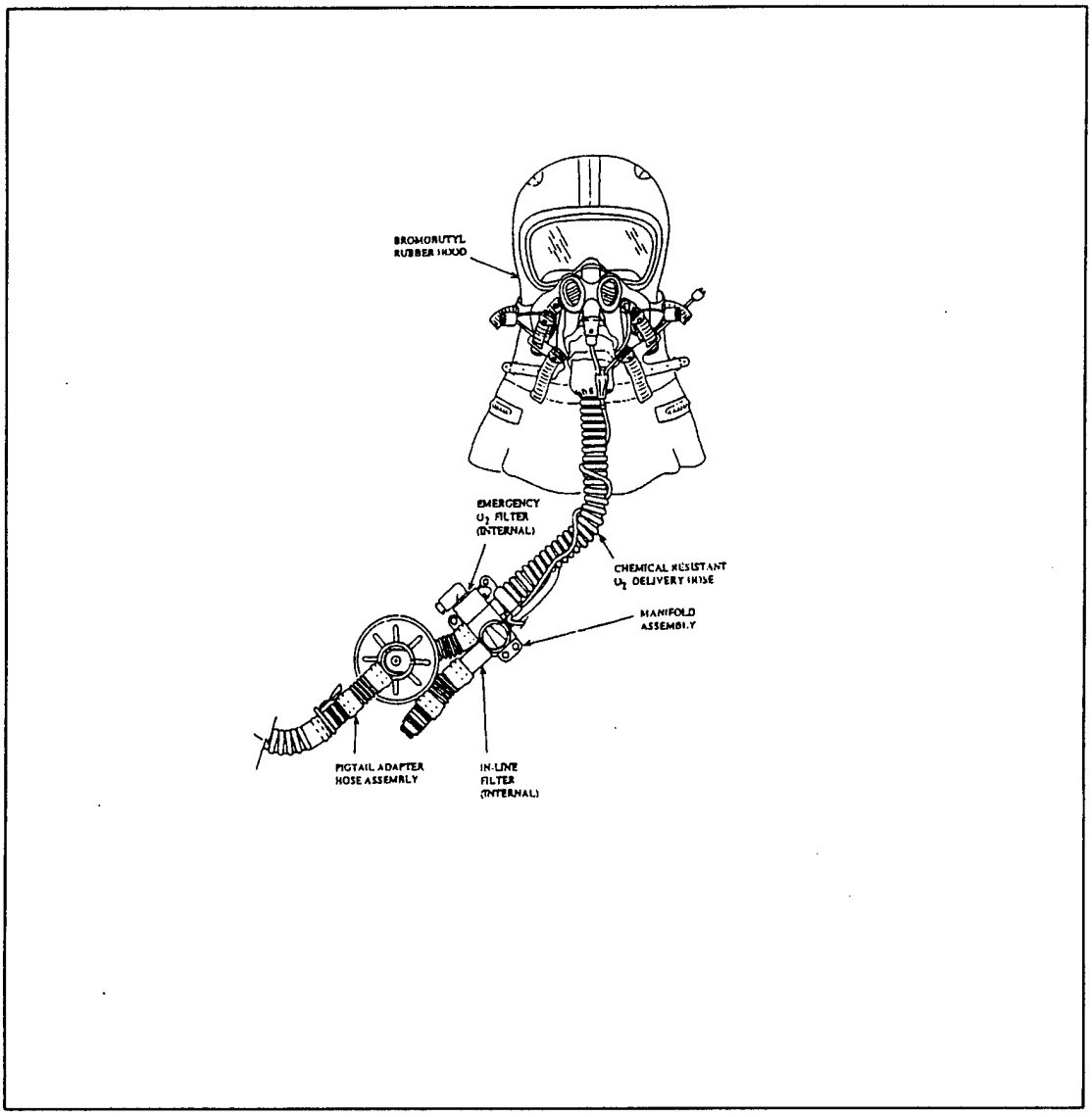

Figure 1.2-2: Rapid Decompression Model Schematic

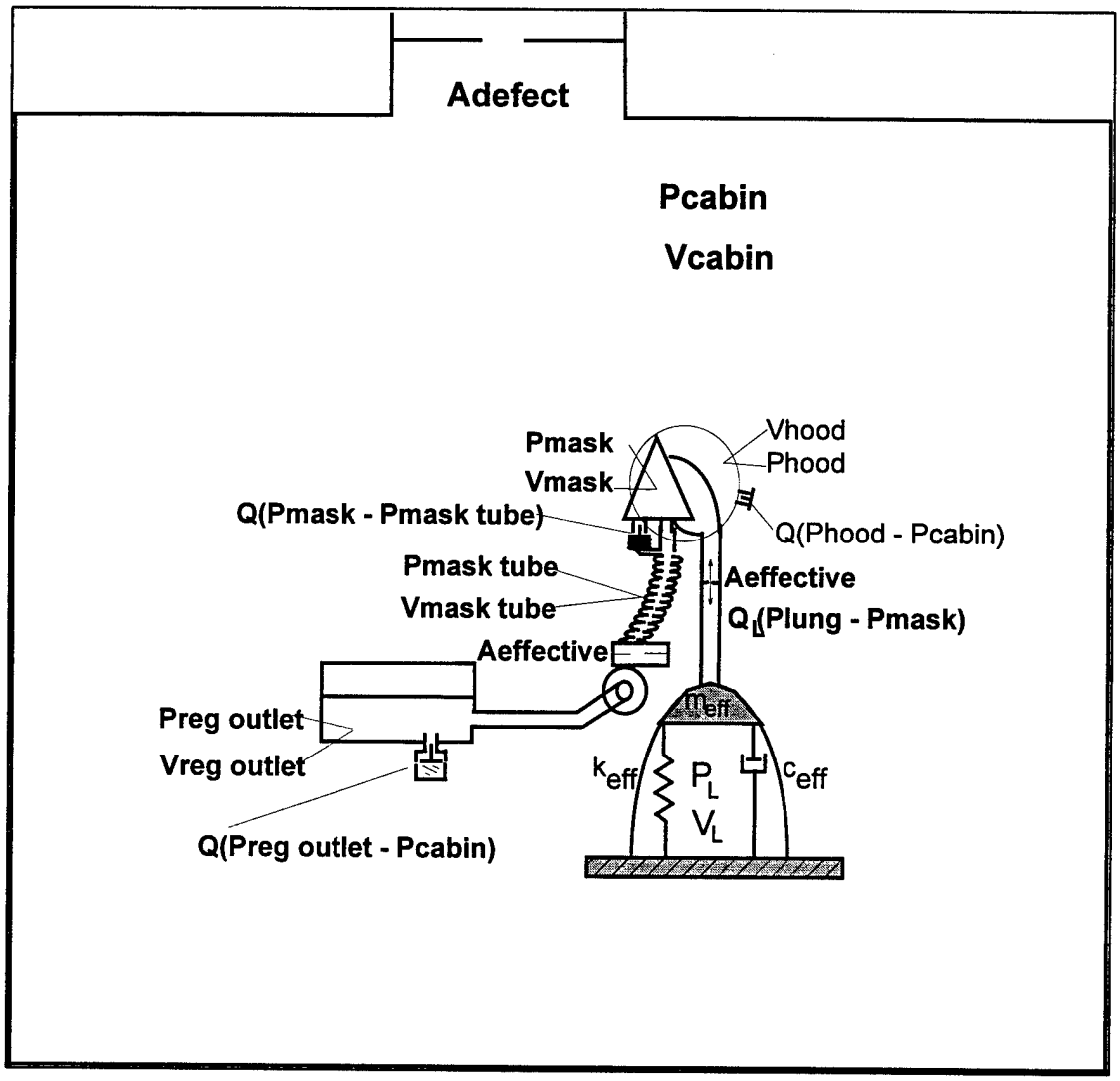

As shown, the AERP System version of the ABS is comprised of the CRU-73 breathing regulator, which is connected via the regulator outlet hose, to the inlet of the MBU-19/P filter canister inlet pigtail. The MBU-12/P mask of the AERP controls the flow of breathing gas into the oronasal cavity and the flow of expired gases out of the oronasal cavity. The lungs, which are modeled as a single compartment, are connected to the oronasal cavity via the trachea. The lungs are represented as an elastic walled compartment whose volume is related to the differential pressure across the lung wall, *i.e.*, the difference in the internal pressure in the lung and the cabin pressure. Normally, this pressure difference is small; however, in a rapid decompression, it is possible for a significant pressure differential to develop across the lung wall

during RD. This high transmural pressure can cause a distension of the thorax and the lungs, which can cause tissue damage in the lung.

1.3 Computer Model. The model, known as the Lung Pressure Transient (LPT) Model was written to run on an IBM compatible personal computer under Microsoft Windows® operating systems. Using the Graphical User Interface (GUI), the user can easily alter values of the controlling parameters without re-compiling the code. Simple graphical plots of the parameters can be created using the user interface. The GUI is primarily designed so that the user can verify the satisfactory completion of a simulation scenario. For more sophisticated analysis, parameter summaries and the results are written to ASCII text files for importing into other applications.

There are two methods for altering the model parameters. The primary method uses the GUI, but for more control, the user can edit the default input file, "default.lpt". This ASCII file is read every time the program is executed and it contains all the parameters for the model to execute. Many of the parameters specified in default.lpt are not available via the GUI. This was done to ensure that the novice user did not change parameters which affect the model stability. However, the expert user can develop different versions of default.lpt using a text editor so that ultimately the user has control over all the parameters, which control the behavior of the program.

Figure 1.3-1 presents a schematic of the program flow of the LPT Model. As shown, the user interacts with the program via a simple GUI, which allows manipulation of a limited set of model parameters, and allows display of the program results. The GUI, interacts with the input files which are read by the Numeric Solver and the output files generated by the Solver.

Figure 1.3-1: Program Schematic

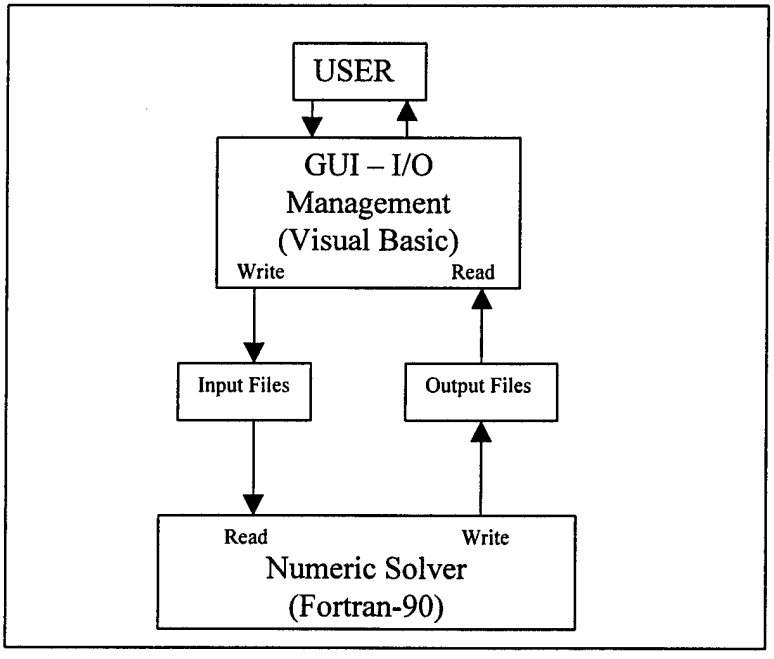

1.4 Simulation Scenarios. All simulations assumed a MILSPEC cabin pressurization schedule with a maximum of 5 psig differential with respect to the prevailing ambient pressure at the specified flight altitude. Other pressure schedules can be investigated by adjusting the maximum cabin differential pressure. BRC modeled the simulation scenarios given in Table 1.4-1. For comparison purposes, simulations without any added breathing equipment resistances were computed for the simulations listed in Table 1.4-1. No attempt was made to model the effects of air flow over the canopy of an aircraft. In this regard, the simulated RD's will be comparable to hypobaric chamber RD, albeit faster. Each simulation was repeated for decompression times of 1.0, 0.5, and 0.1 sec.

Table 1.4-1: Simulation Matrix

PBA (mmHg) / Final Altitude (kft)	0	4	19	30
18	✖			
23	✖			
40		✖		
45			✖	
50				✖

1.5 Assessing Pressure Transients. Data from the literature was employed to judge human tolerance to high transpulmonary pressures. The lung volume data corresponding to static pressures of 80-100 mmHg will be employed as a rough guide to tolerable lung distention.[1,5] It is assumed that even high, short-duration transient pressures will not produce the same distention as that corresponding to the static pressures. The LPT Model incorporates a simple model of the mechanical response of the thorax to dynamic pressure transients which was employed to estimate the distention of the lung by transient pressure pulses computed in Table 1.4-1. This procedure served to produce estimates of the peak pulmonary pressure and lung volume associated with RD to the final altitudes given in Table 1.4-1 of a transient pressure above the nominal 80-100 mmHg criterion. These transients were compared with static pressure-volume relationships previously established by Rahn, et al.[1] to assess their potential for injury.

1.6 Validation. BRC was not in a position to validate the mechanical model of the thorax. Experimental work will be required to verify both peak pressures and thoracic distention. BRC can assist in model revisions based on experimental work, if necessary. However, BRC did employ the model to simulate experiments conducted by Armstrong Laboratories (AL) using a lung simulator. Comparison of the predicted peak pressures computed by the LPT Model and the recorded pressures served to verify that the model was capable of closely predicting the recorded pressures in that experimental set-up for 0.1 second RD's from 8,000 to 23,000 feet and 20,000 to 50,000 feet. The results of these simulations are presented in Section 3.

1.7 Findings and Recommendations. The primary purpose of this project was to analyze the dynamic response of the human respiratory system during rapid decompression as an aid in assigning maximum safe amplitude and duration of mask pressure spikes. As noted above, a mathematical model was created which predicts the dynamic pressure-volume in the lung of an aviator wearing the MBU-19/P AERP Ensemble. The model was employed to predict results of unmanned experiments with which it agreed closely and to predict peak mask and lung pressures in typical decompression scenarios encountered in flight. The following conclusions and recommendations are based on USAF testing, the results of the modeling effort, and a review of the relevant literature.

1.7.1 **Findings.**

a. Inspiratory Path. The inspiratory path volume of the MBU-19/P Ensemble is approximately 165 cm^3 larger than the standard MBU-12/P installation. In addition, there is added resistance to flow (in both directions) associated with the additional hoses, the NBC canister, and the manifold assemblies. The added volume and resistance reduce the rate at which differential pressures, which arise on decompression, can be equilibrated with the environment. Use of longer regulator hoses will exacerbate this effect. Rapid equilibration of mask tube pressures will increase the rate at which the mask and lungs can be equilibrated with the falling cabin pressure during RD.

b. Mask Leakage. The MBU-12/P Oxygen Mask is notorious for leakage at high differential pressures. While this is not desirable during PBA, it does provide a pressure relief effect during rapid decompressions. The MBU-19/P contains an MBU-12/P mask, but the head and mask are enclosed in a hood, which is sealed at the neck. The hood is equipped with a relief valve which appears to be designed to relieve the low flow associated with demisting or blower ventilation of the hood during ground operations. Thus, the relief valve is unlikely to have enough flow capacity to accommodate the mask leakage flows during rapid decompression without a large rise in hood pressure. The pressure retention characteristics of the hood were not determined in the study, but what ever back pressure the hood adds will reduce the rate at which pressure in the mask is able to equilibrate via mask leakage.

c. Computer Model Predictions. The LPT Model's prediction agreed fairly closely with the unmanned experimental RD's conducted at AL/CFT. The highest peak pressures were predicted for short duration RD's at the higher altitudes. The oronasal mask was sealed against leakage in those experiments and, to that extent, they represent worst-case conditions for producing high peak pressures. Additionally they were conducted at a decompression time of 0.1 second. This value was based on an ASCC requirement, but is very high compared to usual manned RD's done to test equipment during man-rating testing. The lung expansions predicted for the MBU-19/P Ensemble were higher than those predicted in simulations without added breathing resistance. However, lung expansions did not seem to be unduly high even when mask and lung peak pressures were high. This is encouraging, but the dynamic response of the lung model employed in the LPT Model is not validated, so that it would be unwise to use those results to infer that the RD's would be safe. It is unfortunate, but taken in total, the modeling results do not

suggest that peak pressures in manned high-altitude 0.1 second RD's would be remarkably different than those seen in the unmanned 0.1 second RD's.

1.7.2 **Recommendations.**

a. Inspiratory Path. Decreases in the volume or the resistance of the MBU-19/P's inspiratory path will improve the ability of the system to equilibrate with the environment and will lower the peak mask pressures seen during RD. This has the additional benefit of reducing the inspiratory path breathing resistance during normal use and it will speed the delivery of oxygen upon loss of cabin pressurization.

b. Regulator Outlet Relief Valve. Use of a compensated relief valve in the breathing regulator outlet or in the inspiratory path of the MBU-19/P will speed equilibration of mask tube pressures with the environment and allow faster mask and lung equilibration during RD.

c. Hood Relief Valve. The flow-pressure characteristics of the hood relief valve and neck seal should be measured to establish the ability of the hood to relieve mask leakage flows during RD and/or PBA. If required, the area of that valve should be increased. The hood volume and compliance should also be measured in ensemble versions at risk of exposure to RD's.

d. MBU-19/P Use Limits. Given the current safety criteria for mask/lung pressure transients, the MBU-19/P should not be routinely worn in flights which expose the system to very rapid RD to altitudes above 40,000 feet. Flight to lower altitudes should be acceptable, with emergency clearance for higher altitudes as necessary.

(1) Aircraft Specific Clearance. With further information, it may be possible to clear the MBU-19/P for specific aircraft. For example, use of the MBU-19/P would be acceptable in aircraft with large volume cabins where the likelihood of a catastrophic loss of cabin pressurization is low. Such aircraft would include most cargo/transport/bomber aircraft. Others might include fighters whose cabin volume is sufficiently large to preclude RD's in less than one second.

(2) Man-rating. The final determination of maximum safe use altitude will require human testing in RD's conducted in hypobaric chambers. A "Build-up" approach should be employed to ensure safety of the test subjects. The Table below offers one approach for starting the series. As each final altitude is safely completed higher altitudes can be explored. The number in each cell indicates the sequence of the RD's.

From Altitude/To Altitude kft Differential Pressure (psig)	8/13 kft 2 psig	8/16 kft 3 psig	8/19.5 kft 4 psig	8/23 kft 5 psig
1.0 sec	1	4	7	10
0.5 sec	2	5	8	11
0.1 sec	3	6	9	12

e. Computer Modeling and Simulation. Computer modeling can be used as a powerful adjunct to the Man-Rating testing. The test results can be used to validate and extend the domain of validity of the model, which in turn can then be employed to predict the results of more hazardous situations where human testing would carry potential risks of injury. Moreover, the modeling and test work could be used to guide the design of breathing system modifications aimed at improving system safety. Once validated, the model could be employed to study the RD performance of other aircrew breathing systems.

2.0 Introduction. This section develops the mathematical relationships necessary to create a model of the ABS. This section was supplied for the interested reader and may be skipped by those who do not wish to review the modeling theory.

2.1 Modeling Pressure-Volume Dynamics. For a stationary system with fixed boundaries, the following mass balance can be written,

$$\left\{\begin{matrix}\textbf{Rate of Mass}\\ \textbf{Accumulation}\end{matrix}\right\} = \left\{\begin{matrix}\textbf{Rate of Mass}\\ \textbf{Inflow}\end{matrix}\right\} - \left\{\begin{matrix}\textbf{Rate of}\\ \textbf{Mass Outflow}\end{matrix}\right\} + \left\{\begin{matrix}\textbf{Rate of}\\ \textbf{Mass Generation}\end{matrix}\right\}.$$

Mathematically,

$$\dot{m} = \frac{d(\rho V)}{dt} = \rho_{in} Q_{in} - \rho_{out} Q_{out} + G(t) \quad . \qquad (1)$$

Where, $\dot{m}$ is the time rate of mass accumulation within the system boundaries, ρ is the bulk density of the material contained within the system volume, V. Q is volumetric flow and $G(t)$ is the time rate of mass generation within the system boundaries. For an ideal gas, the following can be written,

$$\rho = \frac{P}{R_G T} . \qquad (2)$$

Where, P is the absolute pressure in the system, R_G is the specific gas constant for the gas and T is the absolute temperature of the gas. If the temperature is constant, the gas constant is uniform in the inlet and outlet streams and within the system boundary, and there is no mass generation within the system boundaries, then the following equations can be written:

$$\frac{d(V_L P_L)}{dt} = V_L \frac{dP_L}{dt} + P_L \frac{dV_L}{dt} = (\rho_{in} Q_{in} - \rho_{out} Q_{out})(R_G T) \text{ and,} \qquad (3)$$

$$V\frac{dP}{dt} = PQ_{in} - PQ_{out} - P\frac{dV}{dt} = P\left(Q_{in} - Q_{out} - \frac{dV}{dt}\right). \qquad (4)$$

The above can be applied to gas filled systems such as the various components or *compartments* of the Aviator's Breathing System to create a *compartmental model* of the system. The pneumatic flow-pressure laws govern the flows, Q, and the change in the compartment's volume, $\frac{dV}{dt}$, is related to its physical properties and internal pressure. For completely rigid walled

compartments, $\frac{dV}{dt} = 0$. However, for compartments with compliant walls the volume of the compartment changes with flow and pressure according to the following relationship:

$$\Delta P = \frac{1}{\mathbf{C}} \cdot \rho \cdot V + \mathbf{R} \cdot \frac{d\rho \cdot V}{dt} + \mathbf{I} \cdot \frac{d^2 \rho \cdot V}{dt^2}. \qquad (5)$$

Where, **C** is the compartment's compliance, which relates the incremental change in the compartment mass, ρV, per unit of differential pressure change; **R** is the loss of pressure per unit of mass flow within the compartment; and **I** is the pressure loss due to acceleration of mass flow within the compartment. More precisely,

$$\mathbf{C} = \frac{d\rho \cdot V}{dP}, \ \mathbf{R} = \frac{d(\Delta P)}{\frac{d\rho \cdot V}{dt}}, \text{ and } \mathbf{I} = \frac{d(\Delta P)}{\frac{d^2 \rho \cdot V}{dt^2}}, \text{ for linear systems.} \qquad (6)$$

Note that for any real systems the capacitance, resistance, and inductance of the system can be, and usually are, nonlinear. Thus, numerical methods are normally required to solve the differential equations describing the dynamic behavior of pressure and volume in time.

In a compartmental model of a real system, any component can be divided into multiple compartments or more than one component can be combined into a single compartment. The degree of spatial compartmentalization depends on the component's internal structure and the needs of the modeler. For example, to apply the model to a specific compartment, say the human lungs, one can assume that the lung's internal pressure is fairly uniform and the gases are well mixed. This allows the lungs to be modeled as a single compartment. Then one needs, simply, to write the appropriate differential equations and solve them to obtain the pressure and volume relationships in time. For the single compartment lung, the equations are:

$$\frac{dP_L}{dt} = \frac{P_L}{V_L}\left(Q_L - \frac{dV_L}{dt}\right). \qquad (7)$$

Where, Q_L is the *net* volume flow. The sign of Q_L is negative when there is flow out of the lung and positive when there is flow into the lung.

And,

$$\frac{d^2 V_L}{dt^2} = \frac{1}{\mathbf{I}_L} \cdot \left(\frac{\Delta P_L}{\rho_L} - \mathbf{R}_L \cdot \frac{dV_L}{dt} - \frac{1}{\mathbf{C}_L} \cdot V_L\right). \qquad (8)$$

Similar relations can be developed for the other components in the ABS Model. In its present form, the version specific to the MBU-19/P comprises coupled differential equations whose solution describes the pressure, volume, and flow in the various compartments of the model.

2.2 Decompression Dynamics. In the early 1950's, Haber and Clamann[1] developed a practical model for rapid decompression dynamics in connected hypobaric chambers. Rapid decompressions are typically simulated in connected hypobaric chambers by holding the chamber simulating the aircraft cabin to the appropriate cabin pressure and pumping a larger chamber to somewhat below the target final altitude. Once the pressures are stable and the experimental subject is prepared, a large valve between the chambers is opened allowing the gas to flow from the lower altitude chamber (higher pressure) to the higher altitude chamber (lower pressure). Haber and Clamann's model accounted for the rise in pressure in the larger, high altitude, chamber associated with the transfer of air from the smaller, low altitude, chamber. This complication is unnecessary in a model aimed at simulating actual decompressions in aircraft. An aircraft decompresses to an essentially infinite volume, which remains at a constant pressure. This fact allows simplification of the Haber-Clamann Decompression Model[1] as illustrated below. The development follows that of Haber and Clamann in the Appendix to the original paper.

Mass flow through an orifice is given by

$$\frac{d\mathbf{m}}{d\mathbf{t}} = -\rho_A \cdot \mathbf{A} \cdot \mathbf{w}. \qquad (9)$$

Where, **m** is mass, **t** is time, ρ_A is the gas density in the orifice, **A** is the orifice cross sectional area, and w is the velocity of the gas in the orifice.

Also,

$$d\mathbf{m} = d\mathbf{V}_C \rho_C = \mathbf{V}_C \, d\rho_C. \qquad (10)$$

Where, $\mathbf{V}_c$ is the cabin volume, and ρ_c is the density of the gas in the cabin. Further, for a polytropic process, the following holds.

$$\rho_C = \rho_{C0} \cdot \left(\frac{\mathbf{p}_C}{\mathbf{p}_{C0}} \right)^{\frac{1}{k}}. \qquad (11)$$

Where, $\mathbf{p}_C$ is the current pressure, $\mathbf{p}_{C0}$ is the initial pressure, and **k** is the polytropic constant, for example 1.4 for air. Differentiating the equation above yields,

$$dp_C = \frac{1}{k} \cdot \frac{\rho_{C0}}{p_{C0}} \cdot \left(\frac{p_C}{p_{C0}} \right)^{\frac{1-k}{k}} \cdot d\rho_C . \qquad (12)$$

For subcritical pressure ratios, *i.e.* $\frac{p_{C0}}{p_A} < 1.89$, where P_A is the ambient pressure the mass velocity is given by

$$w = \sqrt{\frac{2}{k-1} \cdot k \cdot \frac{p_C}{\rho_C} \cdot \left[1 - \left(\frac{p_A}{p_C} \right)^{\frac{k-1}{k}} \right]} . \qquad (13)$$

The pressure outside the pressure cabin for the above derivation was assumed constant. And, the speed of sound at cabin conditions is given by

$$c_0 = \sqrt{k \cdot \frac{p_{C0}}{\rho_{C0}}} . \qquad (14)$$

Combining the equations above, gives, after manipulation, the expression for the change in cabin pressure as a function of the initial and final conditions, the cabin volume, the orifice area, and the gas properties. For subcritical orifices,

$$\frac{d\left(\frac{p_C}{p_{C0}} \right)}{dt} = - \frac{A \cdot c_0}{V_C} \cdot k \cdot \sqrt{\frac{2}{k-1}} \cdot \left(\frac{p_C}{p_{C0}} \right)^{\frac{k-1}{k}} \cdot \left(\frac{p_A}{p_{C0}} \right)^{\frac{1}{k}} \cdot \sqrt{\left(\frac{p_C}{p_{C0}} \right)^{\frac{k-1}{k}} - \left(\frac{p_A}{p_{C0}} \right)^{\frac{k-1}{k}}} \qquad (15)$$

Setting the time constant, $t_C = \frac{V_C}{A \cdot c_0}$, then,

$$\frac{d\left(\frac{p_C}{p_{C0}} \right)}{d\left(\frac{t}{t_C} \right)} = - k \cdot \sqrt{\frac{2}{k-1}} \cdot \left(\frac{p_C}{p_{C0}} \right)^{\frac{k-1}{k}} \cdot \left(\frac{p_A}{p_{C0}} \right)^{\frac{1}{k}} \cdot \sqrt{\left(\frac{p_C}{p_{C0}} \right)^{\frac{k-1}{k}} - \left(\frac{p_A}{p_{C0}} \right)^{\frac{k-1}{k}}} . \qquad (16)$$

To facilitate integration, Haber and Clamann introduced certain simplifications, which resulted in the definition of the following constants.

$$\mathbf{a} = 1 - \left(\frac{p_A}{p_{C0}}\right)^{\frac{k-1}{k}}, \qquad (17)$$

$$\mathbf{b} = \mathbf{k} - 1, \text{ and } \mathbf{c} = -\frac{1}{2}(\mathbf{k}-1)\cdot(\mathbf{k}-2). \qquad (18)$$

After integration and simplification, an analytical expression for the decompression time, t_E, is obtained.

$$t_E = t_C \cdot \sqrt{\frac{\mathbf{k}-1}{2}} \cdot \frac{1}{\left(\frac{p_A}{p_{C0}}\right)^{\frac{1}{k}} \cdot \sqrt{\mathbf{c}}} \cdot \tan^{-1}\sqrt{4 \cdot \frac{\mathbf{a}\cdot\mathbf{c}}{\mathbf{b}^2}}. \qquad (19)$$

The equation above is valid for decompressions that begin at subcritical pressure ratios *i.e.*,

$\frac{p_{C0}}{p_A} < 1.89$.

For supercritical flow, the mass flow is independent of downstream pressure, so the mass flow is given by,

$$w = \sqrt{2 \cdot \frac{\mathbf{k}}{\mathbf{k}+1} \cdot \frac{p_C}{\rho_C}}. \qquad (20)$$

Then for supercritical flow substitution of this expression for w yields

$$\frac{d\left(\frac{p_C}{p_{C0}}\right)}{d\left(\frac{t}{t_c}\right)} = -\mathbf{k} \cdot \left(\frac{2}{\mathbf{k}+1}\right)^{\frac{k+1}{2(k-1)}} \cdot \left(\frac{p_C}{p_{C0}}\right) \cdot \sqrt{\left(\frac{p_C}{p_{C0}}\right)^{\frac{k-1}{k}}}. \qquad (21)$$

Integration of the above yields,

$$t = t_C \cdot \frac{2}{k+1} \cdot \left(\frac{k+1}{2}\right)^{\frac{k+1}{2(k-1)}} \left[\frac{1}{\left(\frac{p_C}{p_{C0}}\right)^{\frac{k-1}{2k}}} - 1\right]. \qquad (22)$$

Using the following definition for p_{cr}, the critical pressure ratio,

$$p_{cr} = \left(\frac{k+1}{2}\right)^{\frac{k}{k-1}} \cdot, \text{ from which it can be shown that,}$$

$$(p_{cr})^{\frac{k+1}{2k}} = \left(\frac{k+1}{2}\right)^{\frac{k+1}{2(k-1)}}. \qquad (23)$$

Then, finally, the evacuation time, t'_E, during the supercritical phase is given by

$$t'_E = t_C \cdot \frac{2}{k-1} \cdot (p_{cr})^{\frac{k+1}{2k}} \left[\left(\frac{1}{p_{cr} \cdot \frac{p_A}{p_{C0}}} \right)^{\frac{k-1}{2k}} - 1 \right] \qquad (24)$$

However, because the temperature drops during the expansion, it is necessary to modify both the factor, **a**, and the speed of sound, $\mathbf{c_0}$, using the following corrections,

$$\mathbf{a^*} = 1 - \left(\frac{1}{p_{cr}}\right)^{\frac{k-1}{k}}, \text{ and,} \qquad (25)$$

$$\mathbf{c_0^*} = \mathbf{c_0} \cdot \left[p_{cr} \cdot \frac{p_A}{p_{C0}} \right]^{\frac{k-1}{2k}}, \text{ and } t_c^* = \frac{\mathbf{V_C}}{\mathbf{A} \cdot \mathbf{c_0^*}}. \qquad (26)$$

Then, after substitution, integration and simplification, the total decompression time is given for decompressions beginning at or above critical pressure ratios by,

$$t_E = t_c^* \cdot \sqrt{\frac{k-1}{2}} \cdot \frac{1}{\left(\frac{1}{p_{cr}}\right)^{\frac{1}{k}} \cdot \sqrt{c}} \cdot \tan^{-1} \sqrt{4 \cdot \frac{a^* \cdot c}{b^2}} + t_c \cdot \frac{2}{k-1} \cdot p_{cr}^{\frac{k+1}{2k}} \left[\left(\frac{1}{p_{cr} \cdot \frac{p_A}{p_{C0}}} \right)^{\frac{k-1}{2k}} - 1 \right]. \qquad (27)$$

Now, if we define $\mathbf{P_1}$ by $t_E = t_C \cdot P_1$. Which, again, applies for decompressions with initial pressure ratios greater than or equal to $\frac{p_{C0}}{p_A} = \left(\frac{k+1}{2}\right)^{\frac{k}{k-1}}$. For lower pressure ratios, P_1 is defined similarly, but using the expression for $\mathbf{t_E}$ which applies for starting ratios below the critical ratio.

Haber and Clamann[1] conducted a number of experiments to define the temperature change accompanying a rapid decompression. They determined that the polytropic coefficient governing the absolute temperature change was 1.16, which they concluded was reasonable based on thermodynamic considerations. Using their value, absolute temperature changes can be estimated from

$$\frac{T_f}{T_{C0}} = \left(\frac{p_f}{p_{C0}}\right)^{\frac{k-1}{k}}. \qquad (28)$$

Where, T_{C0}, is the absolute temperature in the decompressing space before decompression and T_f, is the final absolute temperature. Also note that the speed of sound varies with the absolute temperature in accordance with the following relationship.

$$\mathbf{c_0 = \sqrt{kR_G T}} \qquad (29)$$

Where, $\mathbf{T}$ is the absolute temperature and $\mathbf{R_G}$ specific gas constant. Using the values for air yields

$\mathbf{c_0 = \sqrt{kR_G T}} = 20.1\sqrt{\mathbf{T}}$, for air with c_0 in m·sec^{-1} and $\mathbf{T}$ in degrees Kelvin.

The modified Haber-Clamann model was incorporated in the LPT Model to model the fall in cabin pressure during rapid decompression.

3.0 Simulation Results. This section presents the results of simulations using the LPT Model. The first series of simulations were designed to verify that the LPT Model could be employed to reasonably predict the experimental results of a series of unmanned rapid decompressions (RD's) reported by the Armstrong Laboratory (AL) in March 1997. The second series of simulations were conducted to predict the pressures and flows, which would occur with a human breathing from the MBU-19/P, connected to the CRU-73.

3.1 Unmanned Testing. The experimental set up consisted of a CRU-73 regulator connected through 36 inches of 0.75-inch regulator outlet hose to either an MBU-12/P Oxygen Mask or an MBU-19/P AERP Ensemble. A metal sealing plate with pressure taps was inserted into the cavity of each mask and sealed with putty. The mask cavity was connected via 40 centimeters of 0.75-inch hose to a Lung Simulator. The Lung Simulator was based on a design supplied by the RAF. It consisted of a 3.5-liter cylinder, which communicates with the attachment hose via a 4.5-mm diameter orifice. The Lung Simulator is designed to offer roughly the same inlet impedance as the normal human respiratory tree.

Pressure recordings of the mask cavity pressure, the regulator outlet pressure and the internal pressure in the Lung Simulator were made during 0.1 second RD's of the system, which was suspended in an altitude chamber. Data from several repetitions of the RD's were averaged to produce means and standard deviations of the peak pressures. These data were summarized in a report, dated 14 March 1997, which was provided to BRC by Lt. Woods of AL.

For the simulations, the LPT Model parameters were set in accordance with those listed for the components in Section 4. Four 0.1 second RD's were simulated, one each of the 12/P and 19/P systems during a simulated 8,000 to 23,000 foot decompression and one each of the two systems during a simulated 20,000 to 50,000 foot decompression. The results are presented below. For each, of the simulations, selected pressure and flow predictions were computed and displayed graphically. For comparison, the means and standard deviations of the peak pressures recorded during the experimental RD's are plotted on the graphs.

3.1.1 MBU-12/P 8,000 to 23,000 feet. See Figures 3.1-1 for pressure predictions and 3.1-2 for the corresponding predicted flows.

3.1.2 MBU-19/P 8,000 to 23,000 feet. See Figures 3.1-3 for pressure predictions and 3.1-4 for the corresponding predicted flows.

3.1.3 MBU-12/P 20,000 to 50,000 feet. See Figures 3.1-5 for pressure predictions and 3.1-6 for the corresponding predicted flows.

3.1.4 MBU-19/P 20,000 to 50,000 feet. See Figures 3.1-7 for pressure predictions and 3.1-8 for the corresponding predicted flows.

Figure 3.1-1: Pressure Prediction for MBU-12/P 8,000 to 23,000 Feet

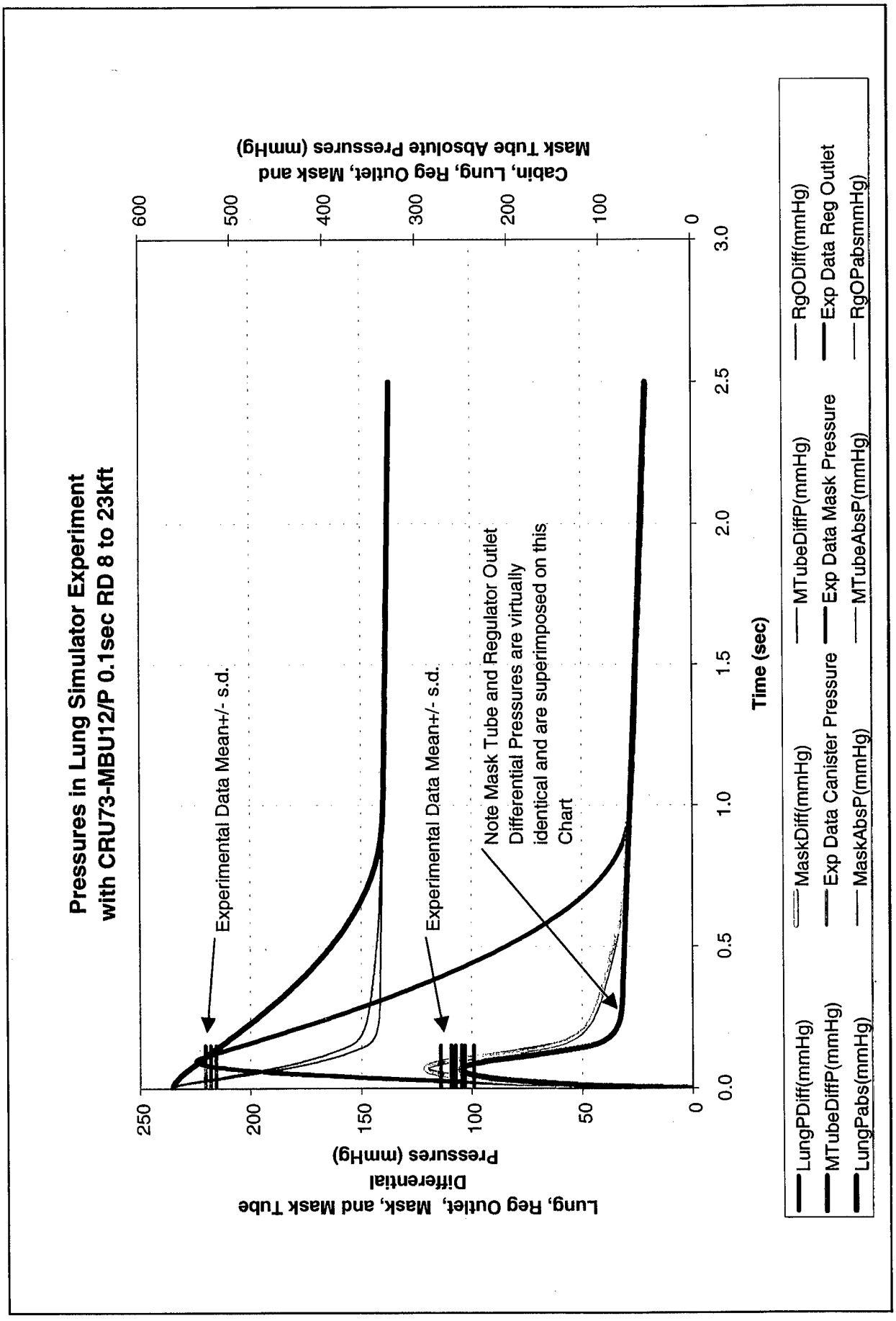

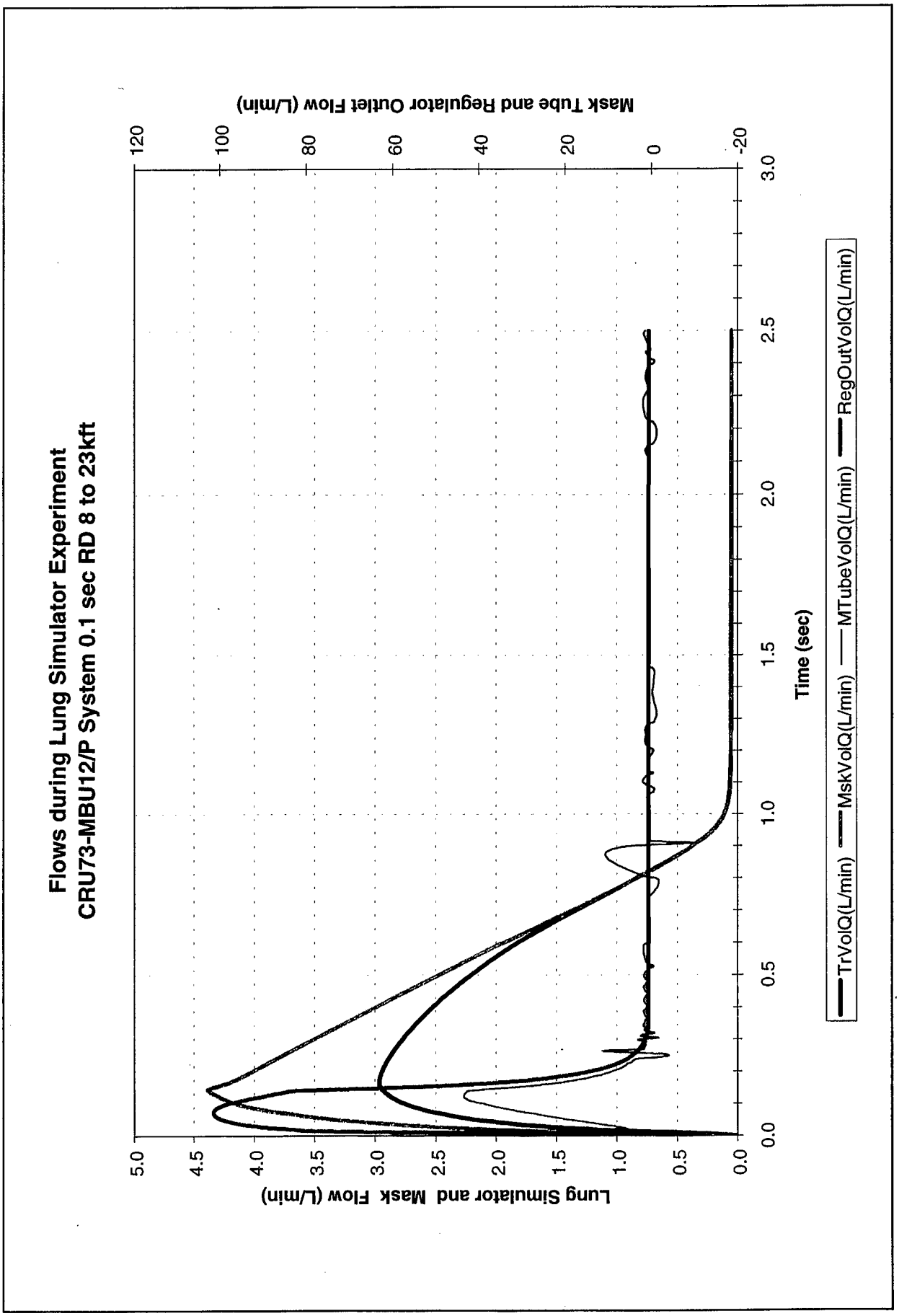

Figure 3.1-2: Flow Prediction for MBU-12/P 8,000 to 23,000 Feet

Figure 3.1-3: Pressure Prediction for MBU-19/P 8,000 to 23,000 Feet

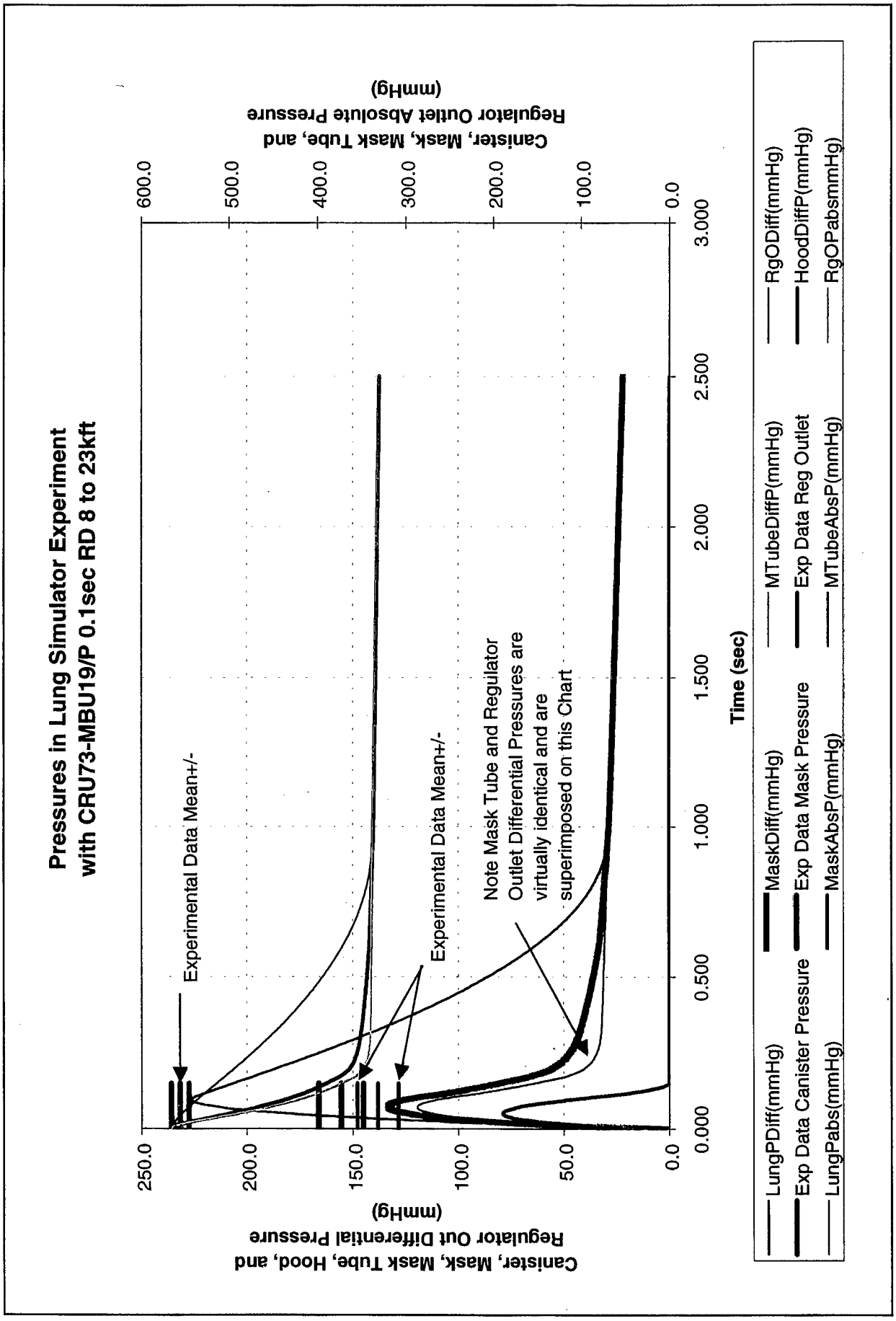

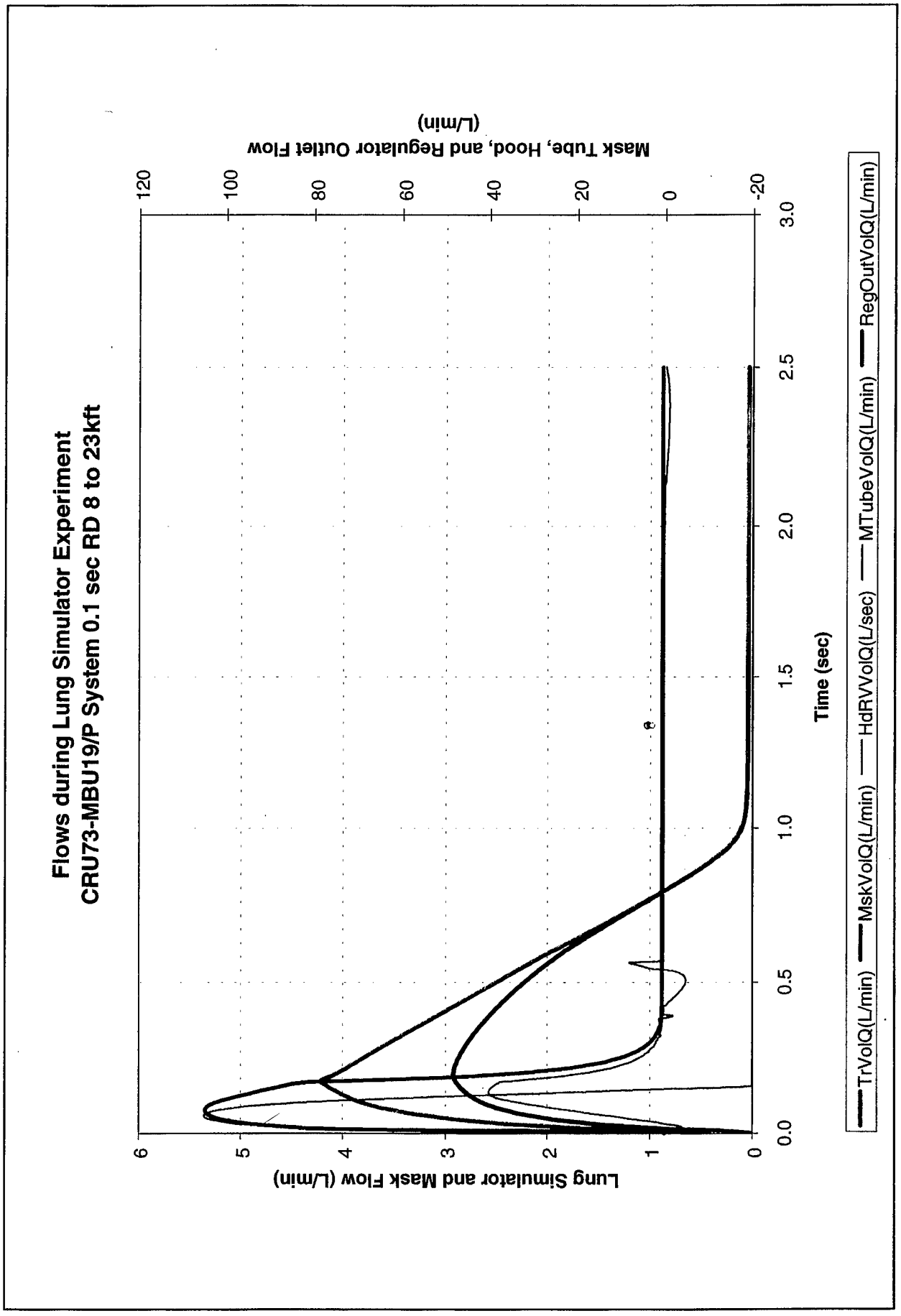

Figure 3.1-4: Flow Prediction for MBU-19/P 8,000 to 23,000 Feet

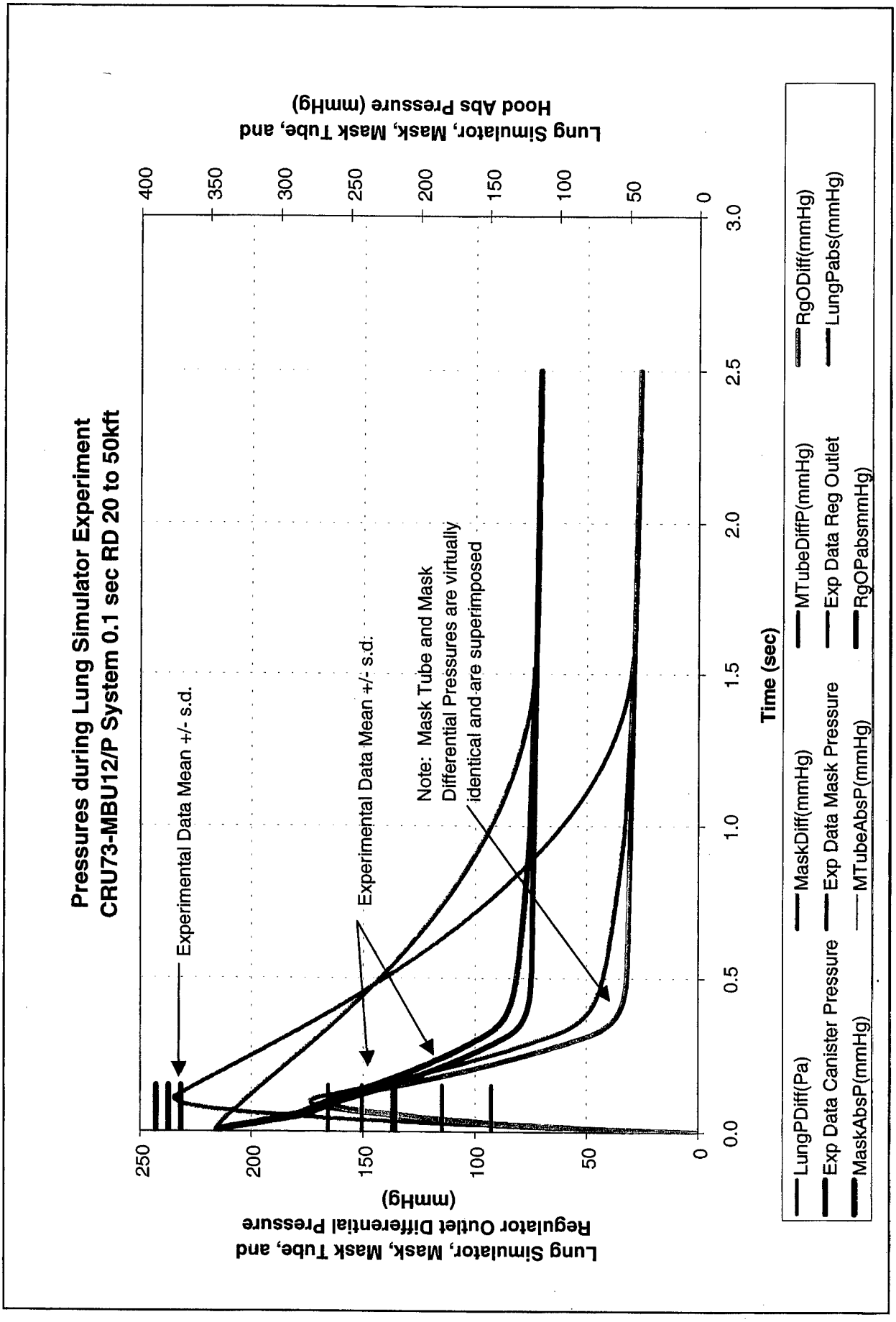

Figure 3.1-5: Pressure Prediction for MBU-12/P 20,000 to 50,000 Feet

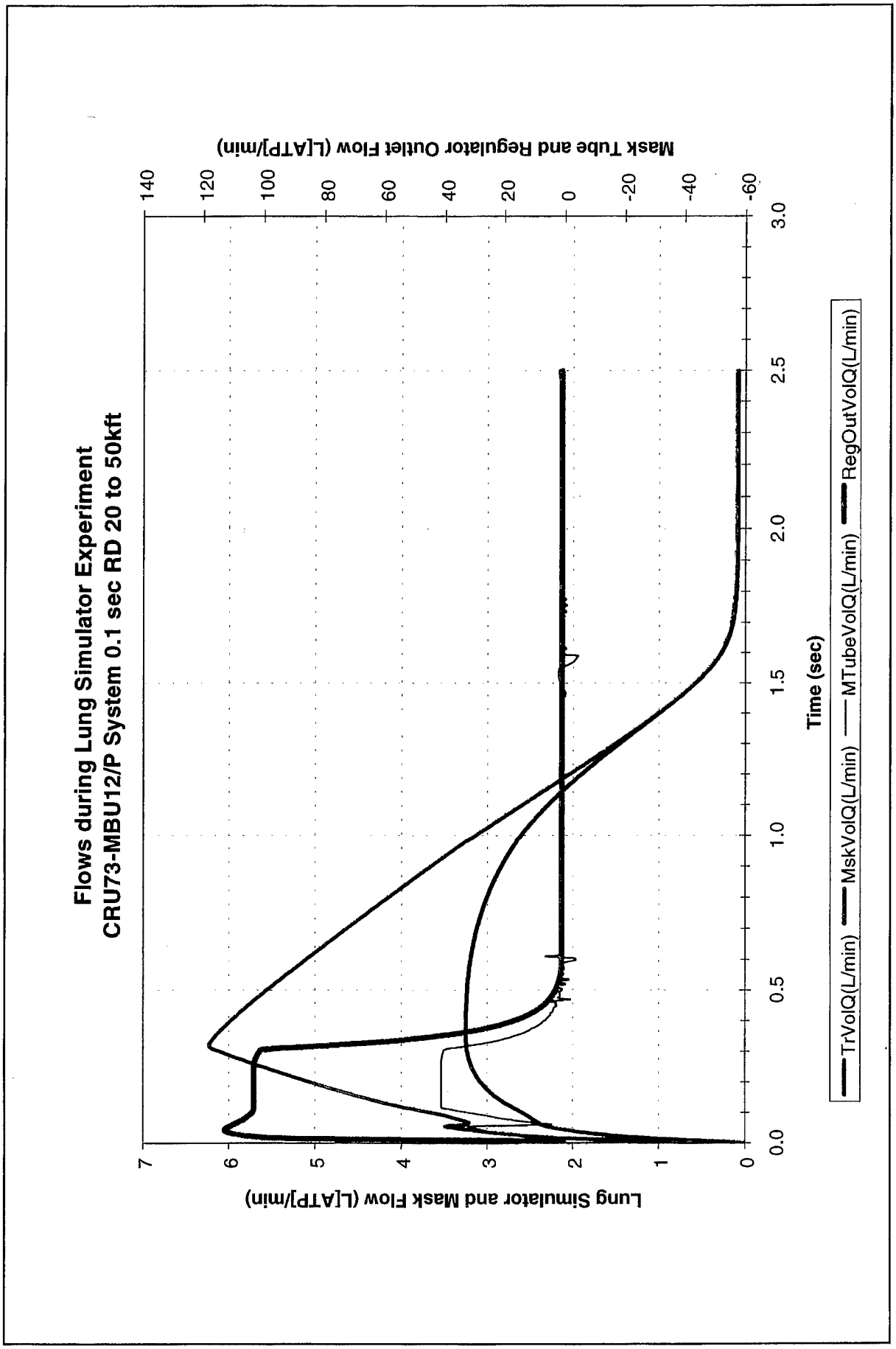

Figure 3.1-6: Flow Prediction for MBU-12/P 20,000 to 50,000 Feet

Figure 3.1-7: Pressure Prediction for MBU-19/P 20,000 to 50,000 Feet

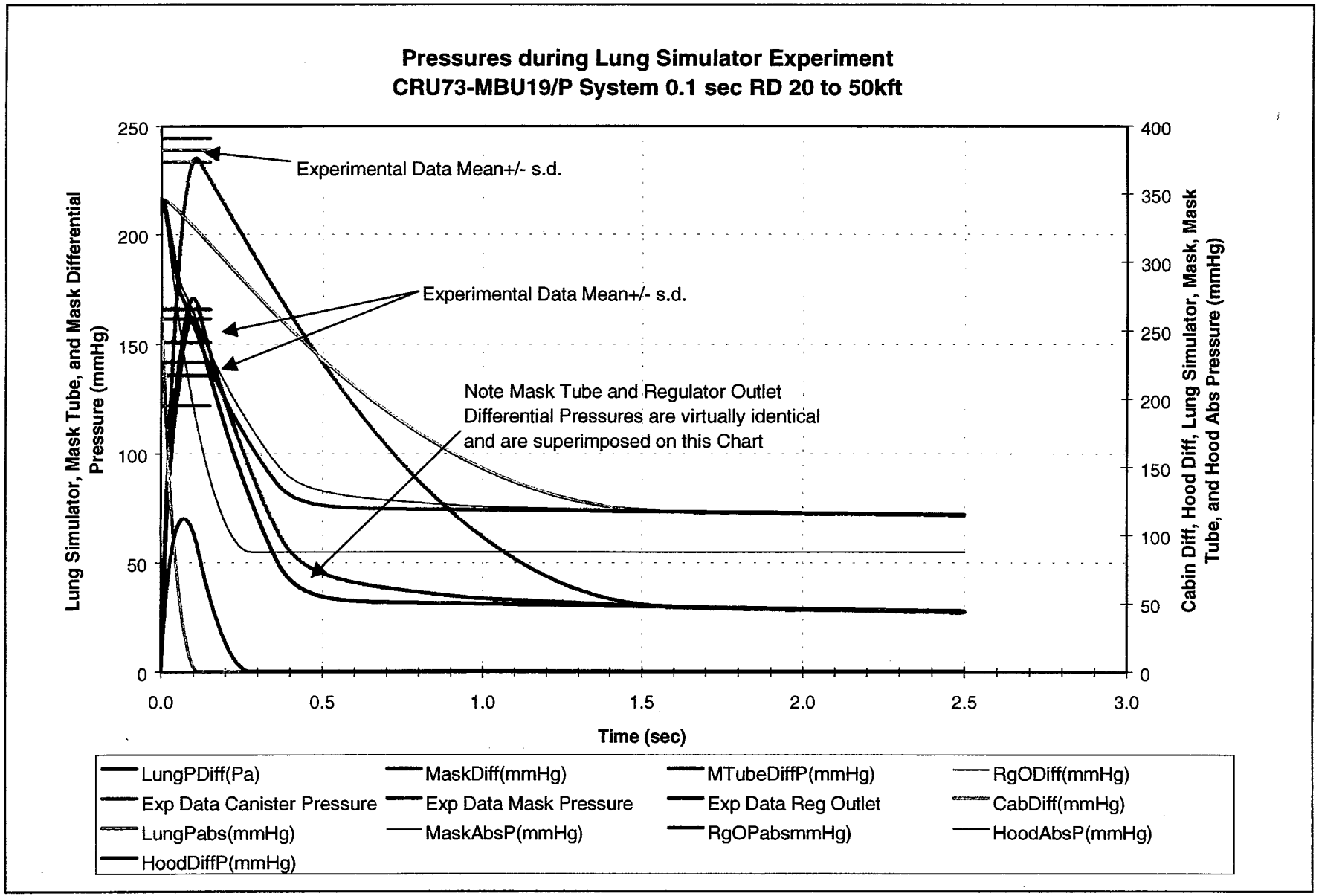

Figure 3.1-8: Flow Prediction for MBU-19/P 20,000 to 50,000 Feet

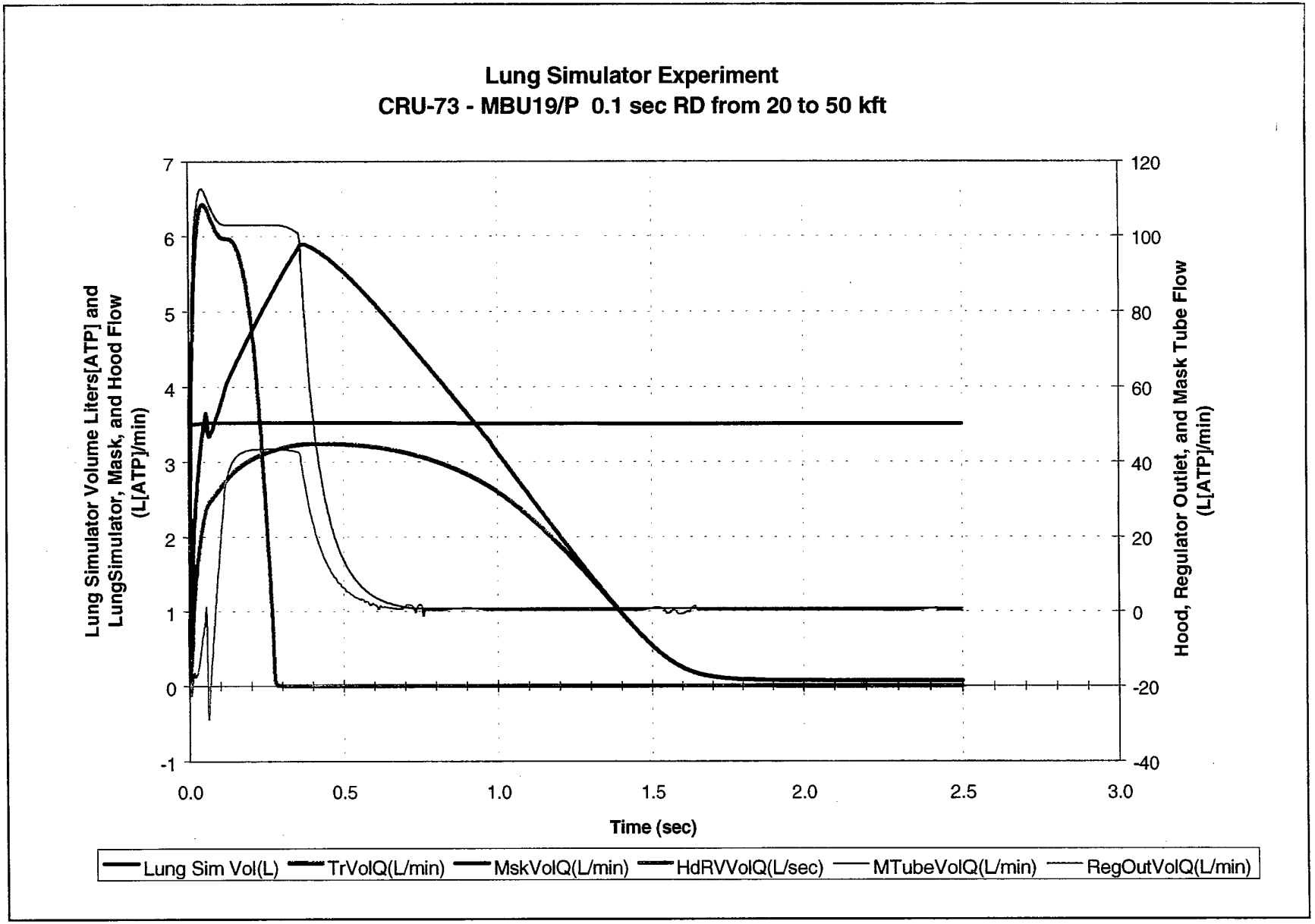

3.2 Project Simulations. Table 3.2-1 summarizes the results of the entire simulation set specified in Table 1.4-1. All simulations were conducted using parameters which represent the MBU-19/P breathing system. Unfortunately, there are no criteria by which to evaluate the safety of the simulated decompressions other than by applying the conventional 80 mmHg peak mask pressure limit. It would be tempting to use the peak lung pressure predictions, however, as the lung model remains invalidated, that would seem unwise.

Table 3.2-1: Summary of MBU-19/P RD Simulation Results

Initial Cabin Altitude (ft)	Final Cabin Altitude (ft)	RD Time (sec)	Peak Mask Pressure (mmHg)	Time above 40 mmHg (sec)	Peak Reg. Outlet Pressure (mmHg)	Peak Lung Pressure (mmHg)	Peak Lung Volume (L)
8,000	18,000	1.0	39	-	37	49	3.4
8,000	18,000	0.5	44	0.27	42	61	3.5
8,000	18,000	0.1	83	0.16	81	86	3.7
8,000	23,000	1.0	44	0.48	41	65	3.6
8,000	23,000	0.5	53	0.36	49	81	3.8
8,000	23,000	0.1	131	0.29	132	120	4.1
16,500	40,000	1.0	46	0.61	43	68	4.3
16,500	40,000	0.5	55	0.45	50	81	4.6
16,500	40,000	0.1	138	0.34	139	113	5.2
18,500	45,000	1.0	46	0.70	44	67	4.6
18,500	45,000	0.5	59	0.46	54	81	5.0
18,500	45,000	0.1	147	0.41	148	112	5.6
20,500	50,000	1.0	47	0.74	44	66	4.9
20,500	50,000	0.5	61	0.49	56	81	5.5
20,500	50,000	0.1	152	0.39	153	110	6.2

For comparison, Table 3.2-2, below, presents simulations that were done without any imposed breathing resistance in the expiratory path. This was accomplished by lowering the regulator outlet poppit valve cracking pressure and enlarging its effective area. This has the effect of removing the compensation pressure at the mask's expiratory valve. Finally, the area of the expiratory valve was enlarged to effectively eliminate its resistance to expiratory flow.

In contrast to the results given in Table 3.2-1, the values given in Table 3.2-2 can be evaluated using Violette's criterion for safety. The second column from the right shows the Violette safety rating. Also shown are the RGE safety ratings suggested by Krebs.[6] Notice that even "safe" decompressions show peak lung pressures over 80 mmHg. This undoubtedly results from the flow limiting nature of the equivalent orifice model of the tracheal resistance.

Table 3.2-2: Summary of RD Simulation Results for Case with No Expiratory Flow Restriction

Initial Cabin Altitude (ft)	Final Cabin Altitude (ft)	RD Time (sec)	Violette Pressure Factor Pi/Pf	Violette Dimensional Factor Vol/Area (m)	Peak Lung Pressure (mmHg)	Peak Lung Volume (L)	Violette Rating (S/U)	Krebs RGE Rating (S/U)
8,000	18,000	1.0	1.5	281	16	3.1	S	S
8,000	18,000	0.5	1.5	140	33	3.2	S	S
8,000	18,000	0.1	1.5	28	73	3.6	S	S
8,000	23,000	1.0	1.8	219	30	3.2	S	S
8,000	23,000	0.5	1.8	110	56	3.5	S	S
8,000	23,000	0.1	1.8	22	101	3.9	S	S
16,500	40,000	1.0	2.8	157	37	3.6	S	S
16,500	40,000	0.5	2.8	78	63	4.2	S	S
16,500	40,000	0.1	2.8	16	96	4.8	S	S
18,500	45,000	1.0	3.3	142	40	3.8	S	S
18,500	45,000	0.5	3.3	71	62	4.5	S	S
18,500	45,000	0.1	3.3	14	96	5.2	U	S
20,500	50,000	1.0	4.0	130	42	4.1	S	S
20,500	50,000	0.5	4.0	65	62	4.9	S	S
20,500	50,000	0.1	4.0	13	96	5.7	U	S

Examples of the time histories calculated for the simulations specified in Table 1.4-1 are illustrated in Figures 3.2-1 to 3.2-10.

Figure 3.2-1: Pressure Prediction for MBU-19/P 16,500 to 40,000

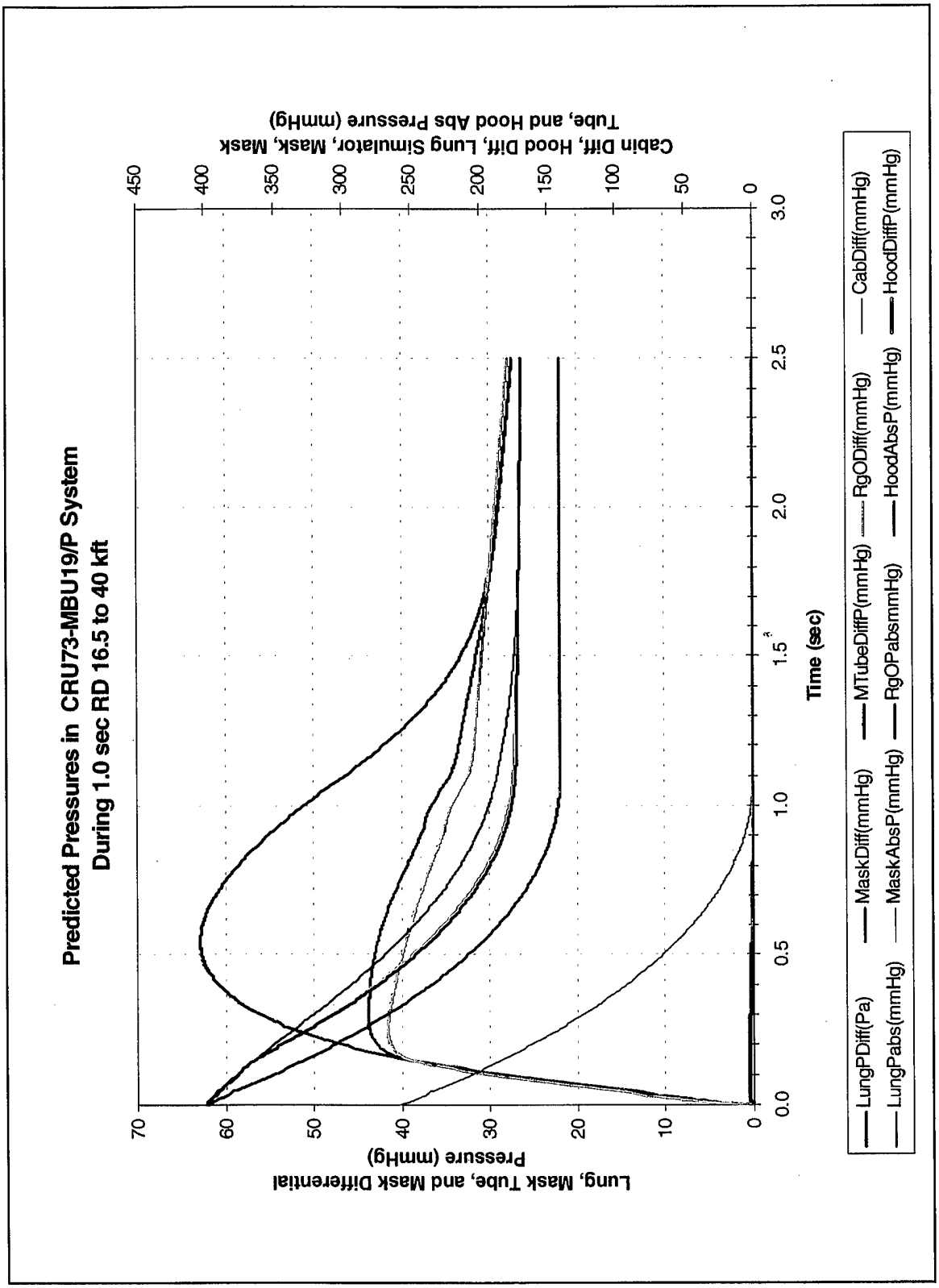

Figure 3.2-2: Flow Prediction for MBU-19/P 16,500 to 40,000

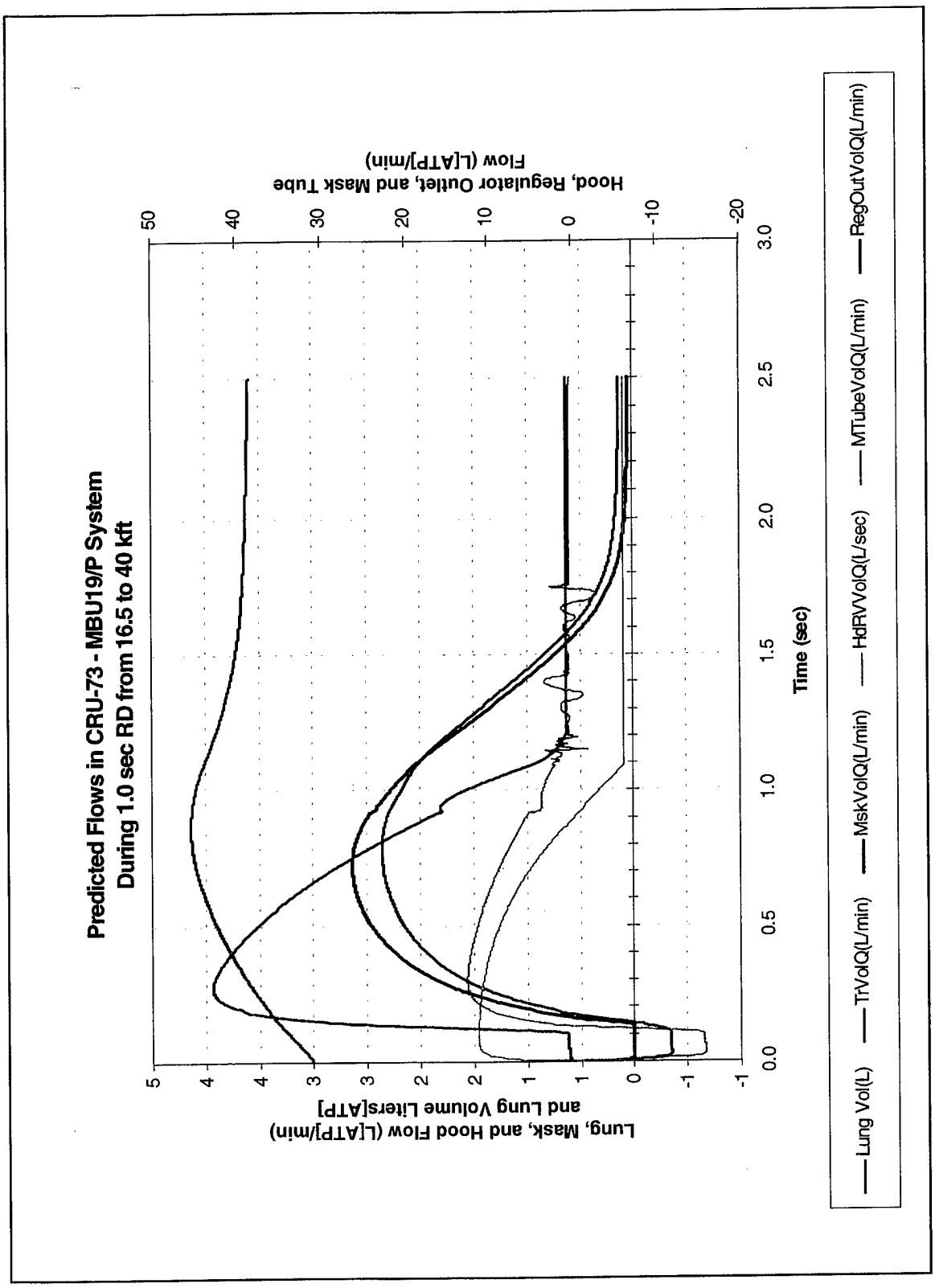

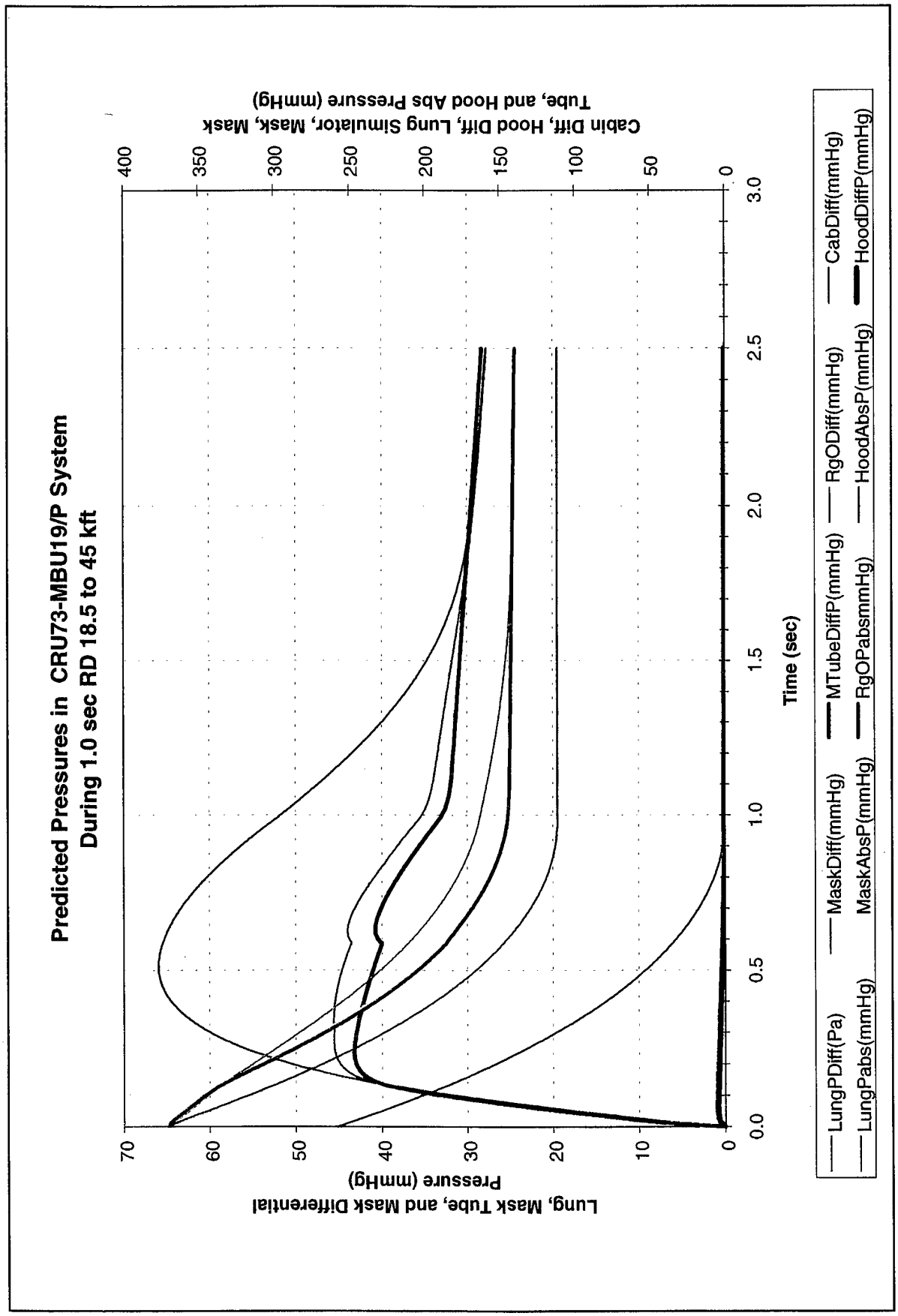

Figure 3.2-3: Pressure Prediction for MBU-19/P 18,500 to 45,000

Figure 3.2-4: Flow Prediction for MBU-19/P 18,500 to 45,000

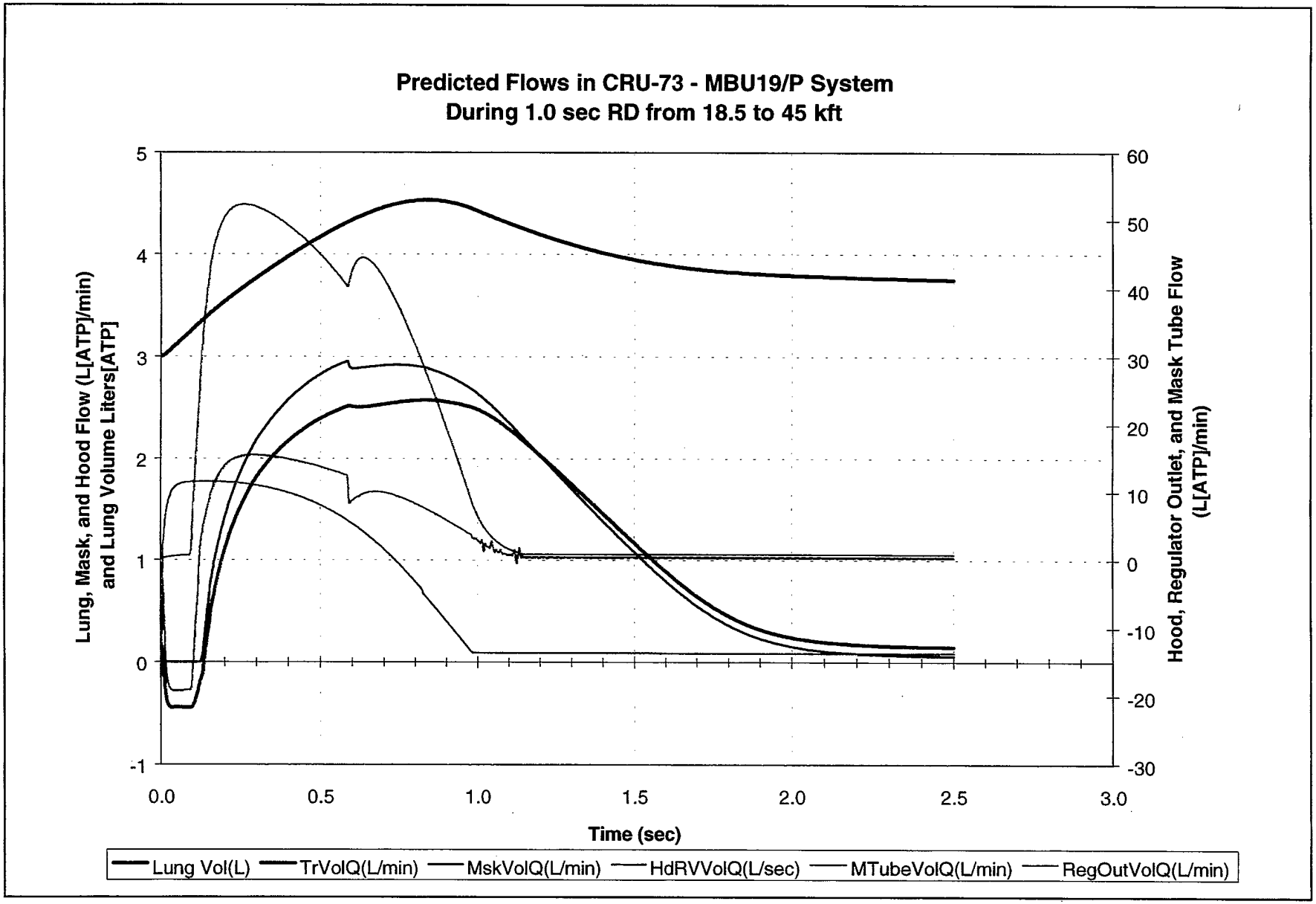

Figure 3.2-5: Pressure Predictions in Human Lung 20,000 to 50,000 Feet

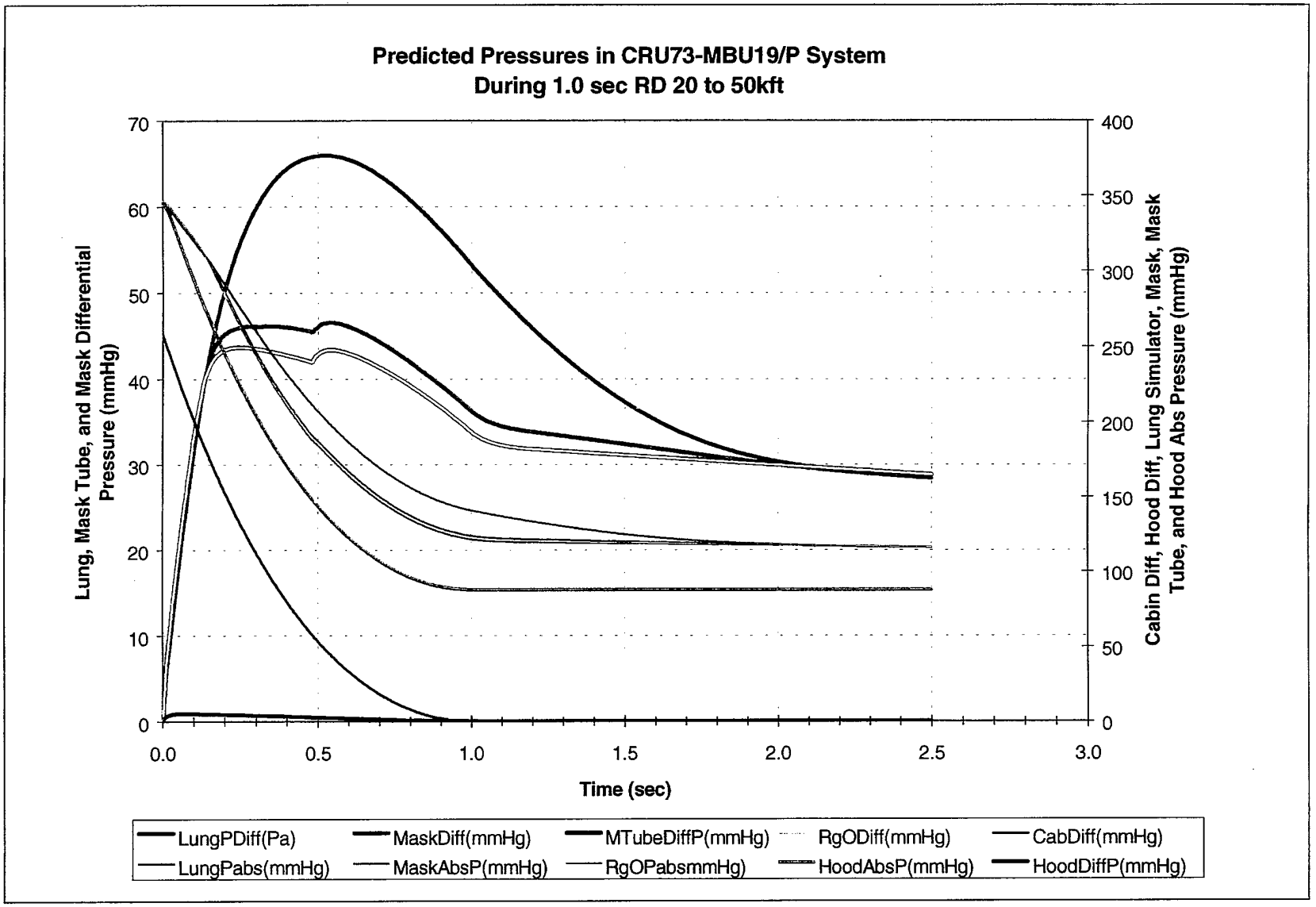

Figure 3.2-6: Flow Prediction for MBU 19/P 2,000 to 50,000 Feet

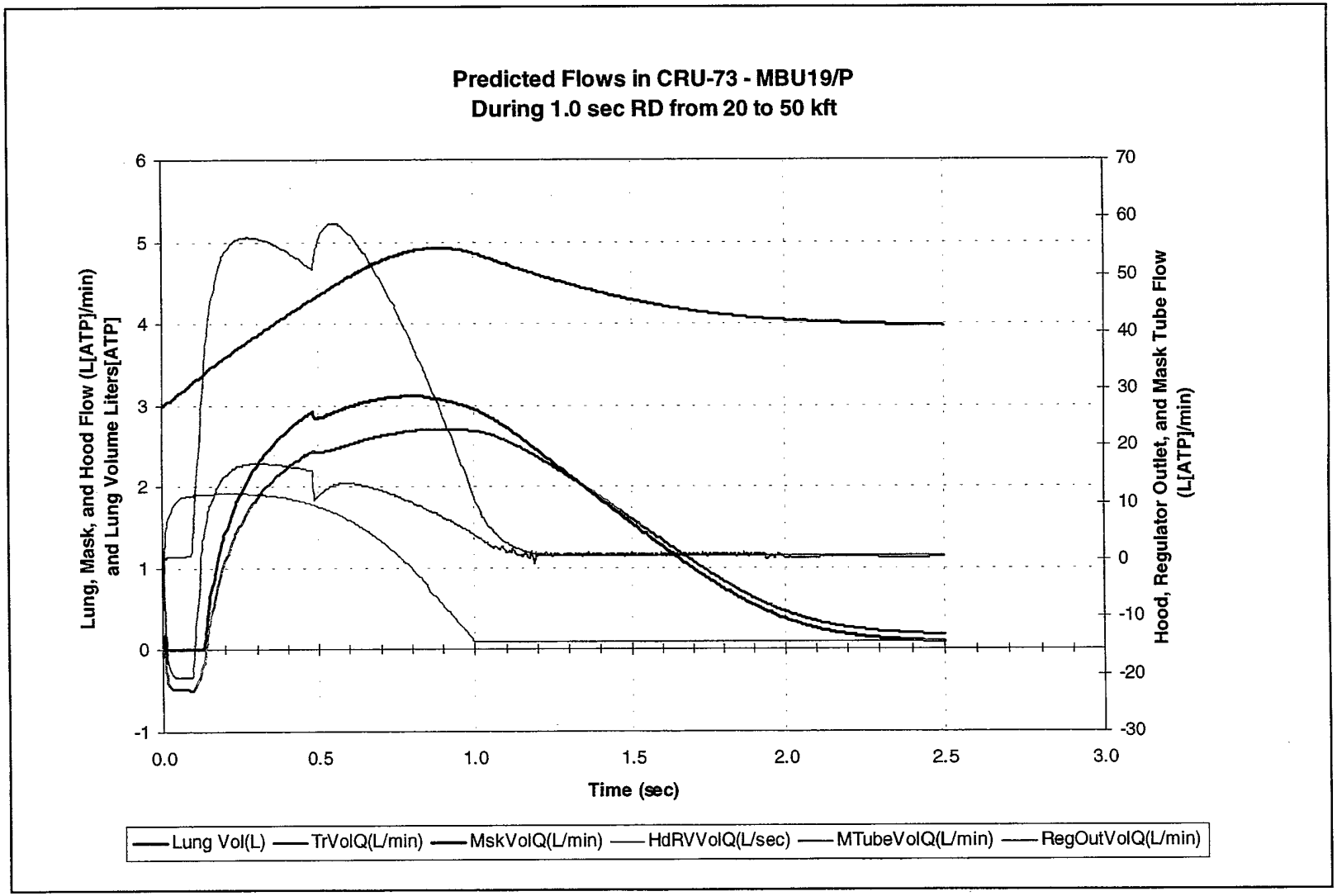

Figure 3.2-7: Pressure Prediction in Human Lung 18,000 to 45,000 Feet

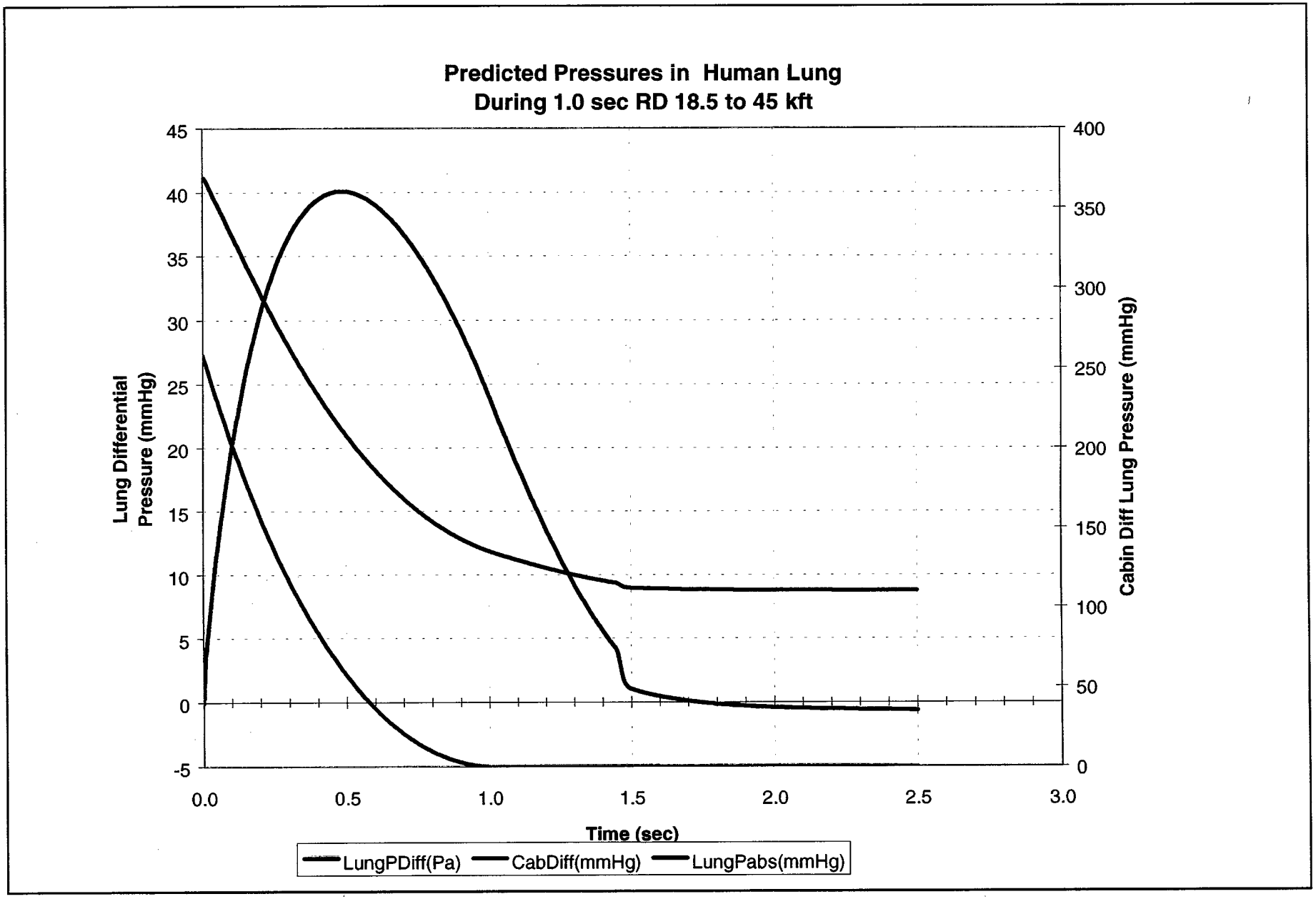

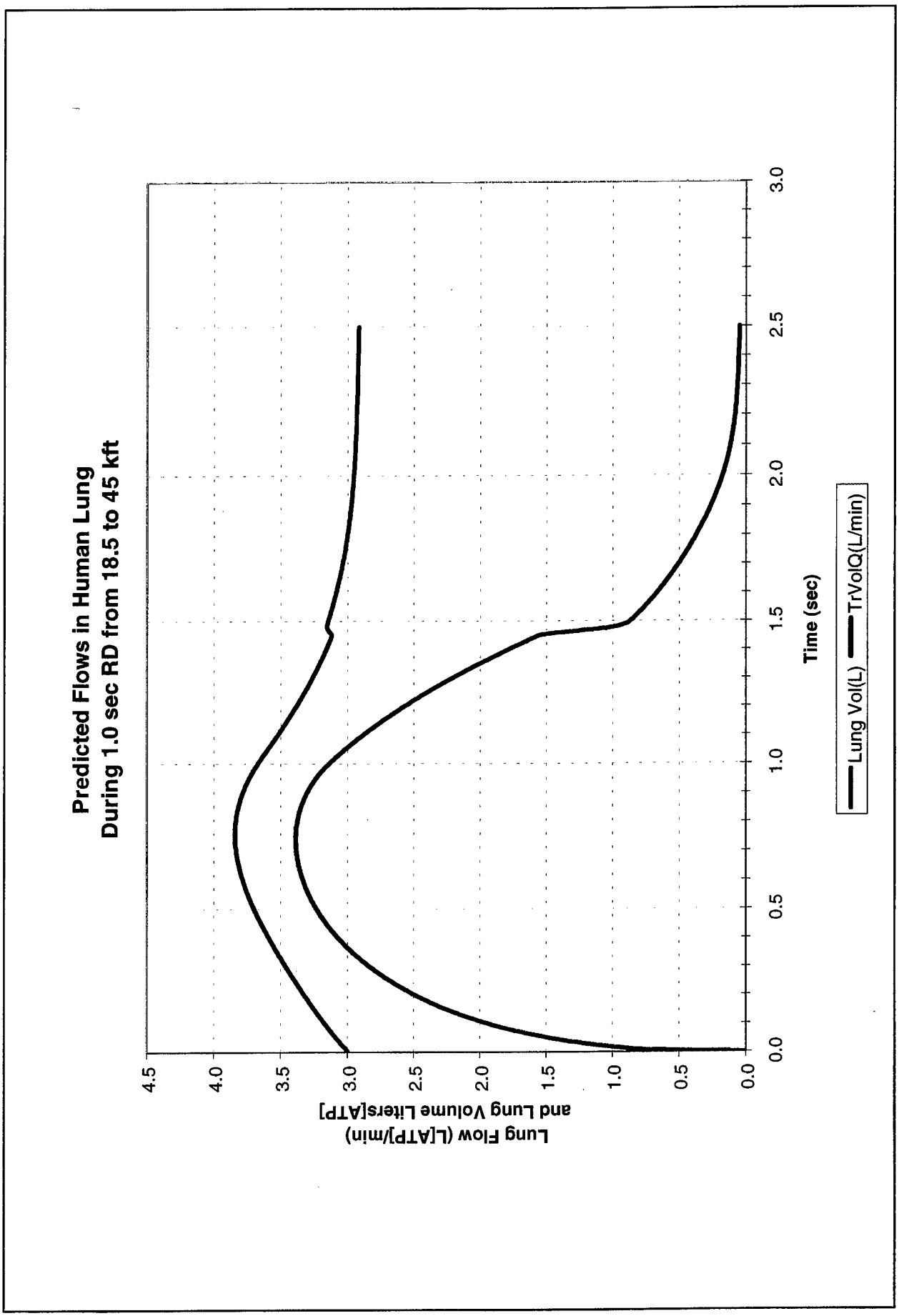

Figure 3.2-8: Flow Prediction in Human Lung 18,500 to 45,000 Feet

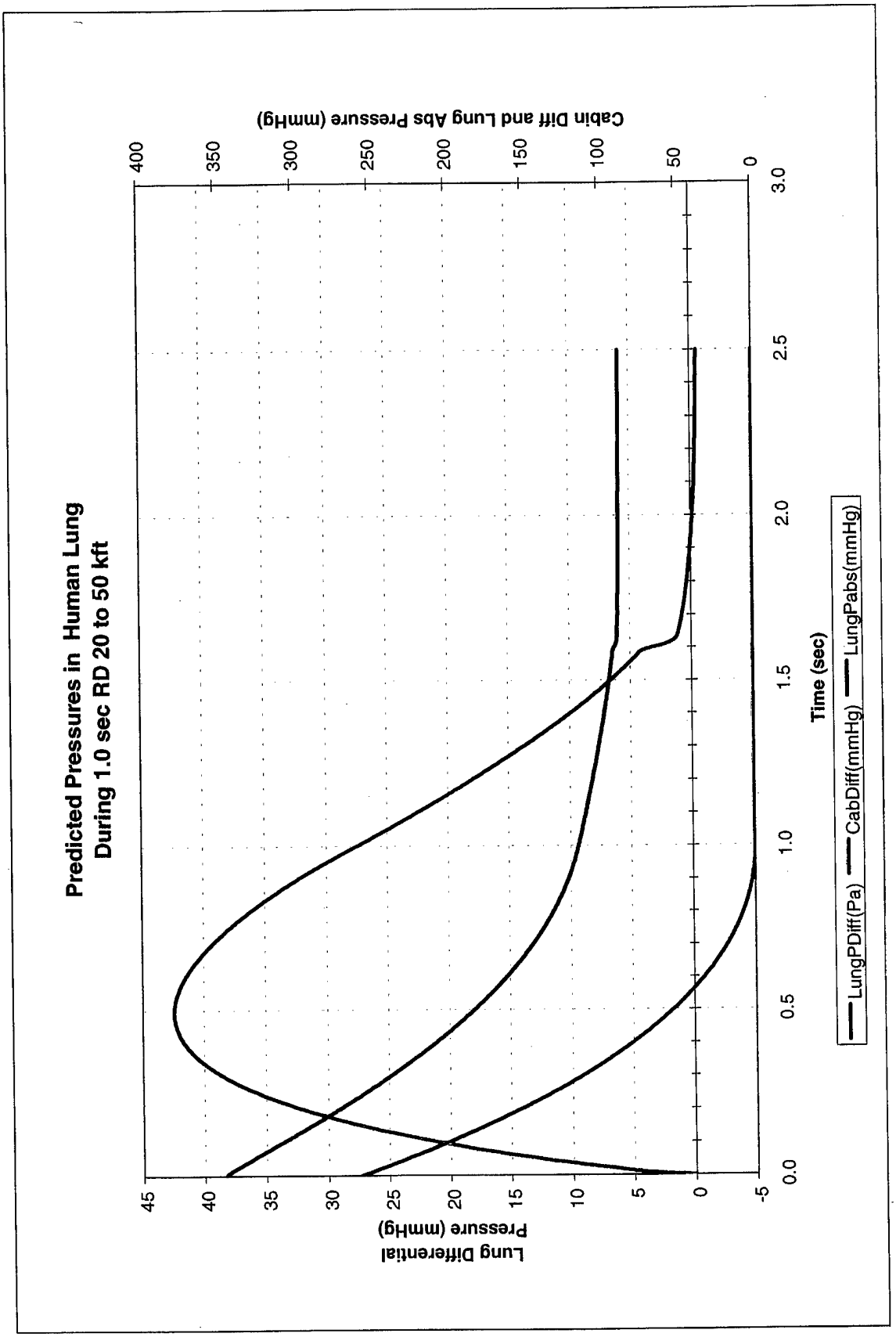

Figure 3.2-9: Pressure Predictions in Human Lung 20,000 to 50,000 Feet

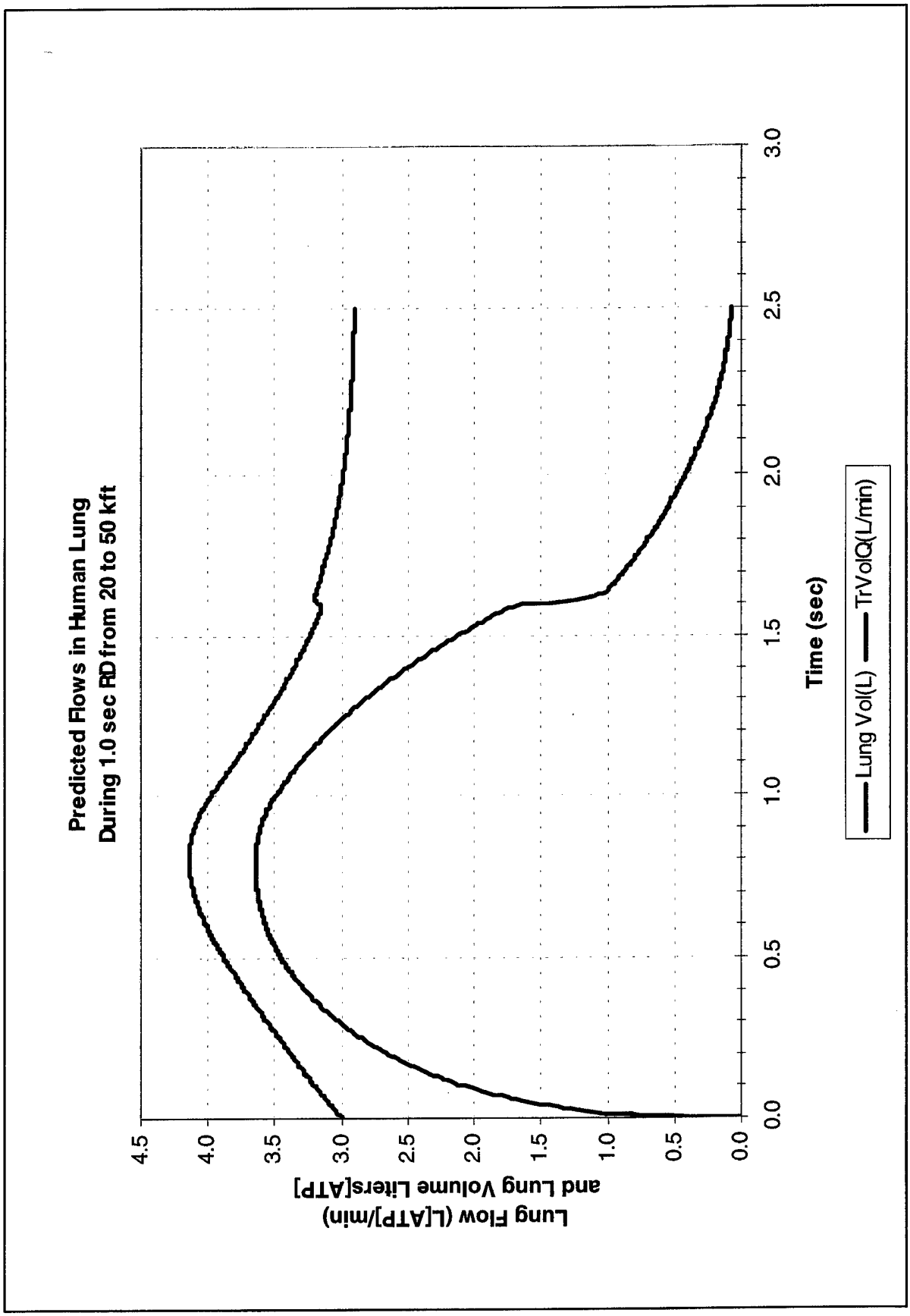

Figure 3.2-10: Flow Prediction in Human Lung 20,000 to 50,000 Feet

4.0 Introduction. Section 4 contains supporting documentation developed during the project. Of primary interest is the Parameter Definition Document, which details the component parameter definitions and their sources. The thoracic pressure-volume diagram is included here as are the analyses employed to determine the pressure-area functions for the regulator outlet and the MBU-12/P expiratory valve.

4.1 Parameter Definitions. The purpose of this section is to summarize the definitions of key model parameters for the Lung Pressure Transient (LPT) Model. The LPT Model will be created specifically to conduct simulations of the transient flows and pressures, which occur in the human lung during rapid decompression (RD) at altitude. The initial aircrew mask to be modeled is the Helmeted version of the USAF MBU-19/P, which is a chemically hardened aircrew breathing mask/hood system with filtration of the inspired gas via a canister-type NBC filter. The breathing regulator employed for this system is the CRU-73. The system includes the necessary hoses to connect the regulator to the MBU-19/P. Mr. T. Van Haasert of Gentex (West) Corporation supplied the attached layout drawings found in Appendix A. It illustrates the major components of the system and their functional layout. A revised model schematic is attached.

4.1.1 Modeled System Definition. This paragraph identifies the major physical components included in the Lung Pressure Transient/MBU-19P Breathing System Model (LPT-19/P) Model. The relevant system components to be included in the model are listed below in order starting at the breathing regulator and ending with the lung. Functionally, the system will be the "Oxygen Flight Operating Mode" as illustrated in Gentex Figure 4-2, attached.

a. Diluter-Demand Regulator. The breathing regulator to be simulated is the standard USAF CRU-73/A. Only the components of the regulator of interest in an RD will be included. These are specifically the outlet relief valve and the volume within the regulator which is vented by that valve.
b. Regulator Outlet Hose. The hose between the outlet of the regulator and the inlet connector to the MBU-19/P.
c. Canister Pigtail. The length of hose between the regulator hose outlet and the canister inlet.
d. NBC Canister. The in-line filter canister between the pigtail and the MBU-19/P manifold inlet hose.
e. MBU-19/P Manifold. The flow path between the canister outlet and the mask tube inlet.
f. Mask Tube. The length of hose leading from the manifold outlet to the inspiratory valve inlet connector.
g. Oxygen Mask. The model will simulate the characteristics of a standard USAF MBU-12/P oronasal mask including its expiratory valve. Mask leakage will be included in the model. The inspiratory valve will not be included in the model.
h. Expiratory Valve Shroud. The vented shroud covering the expiratory valve will be included if its flow resistance contributes significant resistance to outflow from the mask.
i. NBC Hood. The hood enveloping the head will be modeled if its components contribute significantly to outflow resistance from the mask either to mask leakage or to the "normal" expiratory path.

j. Pulmonary System. The oronasal cavity, pharynx, trachea, upper airways, and lung volume will be represented either in lumped or compartmental form as required. The chest wall and diaphragm, as they effect lung expansion, will be simulated. A preliminary lumped parameter model as described by Mead and Milic-Emili[1] will be employed.

4.1.2 Preliminary Parameter Definitions. This section lists the preliminary values for the parameters necessary to model each of the components listed in Section II. In cases where the values are not known precisely, tentative values are assumed. As the model development proceeds, the parameters to which the model is particularly sensitive will be identified.

NOTE: The following are definitions of abbreviations for units and conditions.

V - volume
P - pressure
T - temperature
Q - volume flow
$\dot{m}$ - mass flow
ATA - Atmospheres absolute (pressure)
ATPD - Ambient Temperature and Pressure Dry
BTPS - Body Temperature and Pressure Saturated (37°C, pH_2O = 47mmHg, at the prevailing pressure at the point of interest).
NTPD - Normal Temperature and Pressure Dry (15°C, 1 ATA)
STPD - Standard Temperature and Pressure Dry (0°C, 1 ATA)
mmHg - millimeters of Mercury (pressure)
inWG - inches Water Gauge (pressure)
L - liters (volume)
min - minutes
sec - seconds
in - inches (length)
cm - centimeters (length)
m - meters (length)
psig - pounds(force) per square inch gauge (pressure)
psia - pounds(force) per square inch absolute (pressure)
Pa - Pascal

[1] Mead, J. and Milic-Emilic, J. Theory and methodology in respiratory mechanics with glossary of symbols. Handbook of Physiology, Respiration IV. Chapter 11:363-376. (1981).

1.1.1. Diluter-demand Regulator. These values are based on the MILSPEC dated 10 Feb 81. Mr. Victor Chrome of Litton recommended we use MIL-R-83178, as amended.

1.1.1.1.1. Outlet Volume. $V_{RO} \approx 45\ cm^3 = 2.75\ in^3$ (Estimate provided by Mr. Chrome).

1.1.1.1.2. Cracking Pressure. $P_{RVCP} \approx 17\ inH_2O = 31.8\ mmHg$

1.1.1.1.3. Full Open Pressure. $P_{RVFO} \approx 0.98\ psig = 50.8\ mmHg$

1.1.1.1.4. Flow when fully open $Q_{FO} \approx 45\ L \cdot min^{-1}$ @ NTP D

1.1.1.1.5. Effective Area. $A_{RV} \approx 0.104\ cm^2$.

1.1.2. Regulator Outlet Hose. These values will vary with the configuration of the regulator installation. The USAF is to provide the final values for the model.

1.1.2.1.1. Length. $l_{RH} \approx 36\ in = 0.91\ m$

1.1.2.1.2. Effective Diameter. $d_{RH} \approx 0.75\ in = 1.91cm$

1.1.2.1.3. Volume. $V_{RH} \approx 0.47\ L = 4.7 \cdot 10^{-4}\ m^3$

1.1.2.1.4. Flow Resistance. A quadratic flow pressure relationship was estimated from theoretical flow-pressure models. The model employed is $\Delta P = 1.74 \cdot 10^4 Q + 2.62 \cdot 10^7 Q^2$. Where, ΔP is given in Pascals and Q is given in $meters^3 \cdot sec^{-1}$.

1.1.3. Canister Pigtail Adapter.

1.1.3.1.1. Length. $l_{CP} \approx 6\ in = 15\ cm$

1.1.3.1.2. Effective Diameter. $d_{CP} \approx 0.75\ in = 1.91\ cm$

1.1.3.1.3. Flow Resistance. A quadratic flow pressure relationship was estimated from theoretical flow-pressure models. The model employed is $\Delta P = 1.74 \cdot 10^4 Q + 2.62 \cdot 10^7 Q^2$. Where, ΔP is given in Pascals and Q is given in $meters^3 \cdot sec^{-1}$.

1.1.4. Canister. These values were supplied by Racal to Lt. Woods.

1.1.4.1.1. Volume. $V_{CT} \approx$ Total $= 4.91\ cm^3 = 80.5\ cm^3$, Charcoal Volume $= 2.14\ in^3 = 35\ cm^3$, and Void Volume, $V_{CV} = 2.77\ in^3 = 45.5\ cm^3$.

1.1.4.2. Flow Resistance. $R_C \approx 5. \times 10^{-2}\ mmHg \cdot L^{-1} \cdot min$ NTP D (linear). (This is equivalent to approximately 5.4 inWG at 200 $L^{-1} \cdot min^{-1}$ NTP D or 666 Pa at $3.33 \cdot 10^{-3}\ m^3 \cdot sec^{-1}$)

1.1.5. MBU-19/P Manifold.

1.1.5.1.1. Volume. $V_{CM} \approx 40\ cm^3$.(per measurements at BAFB)

1.1.5.1.2. Flow Resistance. $R_C \approx 1.0 \times 10^{-2}\ mmHg \cdot L^{-1} \cdot min^{-1}$ NTP D (linear). (This is equivalent to approximately 1 inWG at 200 $L^{-1} \cdot min^{-1}$ NTP D or 249 Pa at $3.33 \cdot 10^{-3}\ m^3 \cdot sec^{-1}$.)

1.1.6. Mask Tube. Gentex West supplied the value for volume.

1.1.6.1.1. Volume. $V_{MT} \approx 174\ cm^3$.

1.1.6.1.2. Diameter. $d_{MT} \approx 0.75\ in = 1.9\ cm$.

1.1.6.1.3. Length. $l_{MT} \approx 61\ cm$.

1.1.6.2. Flow Resistance. A quadratic fit to unpublished laboratory data was employed to create the following flow vs pressure loss model. $\Delta P = 7.5 \cdot 10^3 Q + 4.5 \cdot 10^6 Q^2$. Where, ΔP is given in Pascals and Q is given in $meters^3 \cdot sec^{-1}$.

1.1.7. Oxygen Mask. Gentex West supplied the values for volume and flow resistance. Additional flow resistance data were taken from unpublished laboratory data available to Dr. J. Bomar.

1.1.7.1. Mask Deadspace. $V_M \approx 230$ cm^3

1.1.7.2. Expiratory Valve Flow Resistance.

1.1.7.2.1.1. Cracking Pressure. $P_{MXVCP} = 0.0$ Pa

1.1.7.2.1.2. Maximum Area. $A_{MMXV} = 7.0 \cdot 10^{-5}$ m^2.

1.1.7.2.1.3. Pressure required to reach A_{MMXV}. $P_{MMXV} = 450$ Pa

1.1.7.3. Mask Leakage. (These are estimated values).

1.1.7.3.1.1. Maximum Sealing Pressure. $P_{MLSM} \approx 4000$ Pa

1.1.7.3.1.2. Seal Failure Pressure. $P_{MLSF} \approx 8000$ Pa

1.1.7.3.1.3. Flow with seal failed. $Q_{MLSF} = 1.67$ m$^3 \cdot$sec^{-1}

1.1.7.4. Expiratory Valve Shroud.

1.1.7.4.1. Effective Volume. $V_{EVS} \approx 198$ cm^3 (per measurements at BAFB)

1.1.7.4.2. Flow Resistance of Shroud Vents. Negligible

1.1.8. NBC Hood.

1.1.8.1.1. Effective Volume with Helmet. $V_H \approx 1$ L (estimate).

1.1.8.1.2. Relief Valve Cracking Pressure. $\Delta P_{HRVCP} = 0.1$ inWG.

1.1.8.1.3. Relief Valve Flow Resistance. $\Delta P_{HRV}(\dot{m}, A_{RV}, C_D) = 0.1$ inWG at 20 L$^{-1} \cdot$min^{-1} NTP D[1]. (per estimate by Mr. J. Damron, ILC Dover)

1.1.9. Pulmonary System. The values chosen for lung volumes and flow resistance were determined from published references as given below.

1.1.9.1.1. Anatomic Deadspace Volume. $V_D \approx 150$ cm^3

1.1.9.1.2. Lung Volume (End Inspiratory Volume). $V_{LEIV} \approx 3{,}000$ cm^3.

1.1.9.1.3. Vital Capacity $V_{LVC} \approx 4{,}500$ cm^3.

1.1.9.1.4. Residual Volume. $V_{LRV} \approx 1{,}500$ cm^3.

1.1.9.1.5. Total Lung Capacity. $V_{LTLC} \approx 6{,}000$ cm^3.

1.1.9.1.6. Effective Cross Sectional Area of Trachea. $A_T^2 \approx 0.2$ cm^2 (effective diameter ≈ 5 mm)

1.1.9.1.7. Flow Resistance of Upper Airways. The upper airway flow resistance will be approximated using a "lumped parameter model" by employing an orifice model using the area dimensions given above. Distributed resistance models are available *e.g.*, see Weibel[3]. However, such models are computationally complex and the lumped parameter model will be employed unless it is determined that the internal flow resistance of the lung contributes significantly to transmural pressure developed across the thorax during RD.

---

[2] Value for effective cross sectional area of trachea was taken from Luft and Bancroft. Transthoracic Pressure in Man during Rapid Decompression. Aviation Medicine, Jun 1956:208-220. The value actually given was the effective diameter of the orifice equivalent of the trachea. Their value, 4.78 mm, was a calculated average of 7 experimentally determined values.

[3] Weibel, E.R. Morphometry of the Human Lungs. Springer-Verlag (Berlin), (1963).

1.1.9.2. Chest Wall. For the purposes of setting the upper allowable limit for hazardous lung/chest expansion, the static P-V diagram will be employed. Rahn, et al[4], gave an example of such a P-V diagram.

1.1.9.3. Diaphragm. The compliance of the diaphragm will be lumped with the chest wall compliance unless it is found necessary to model the diaphragm's compliance separately.

1.1.9.4. Dynamic Expansion of the Thorax. The model of Mead and Milic-Emili[1] will be employed. Their model is a second order lumped parameter model of the form, $\dot{P} = L\ddot{Q} + R\dot{Q} + \frac{1}{C}Q$. Where, P is differential pressure, Q is volume, R is flow resistance, L is flow inertance, and C is capacitance. The dots indicate derivatives of the quantities with respect to time.

1.1.9.4.1. $L \approx 1.2 \cdot 10^{3}\ Pa \cdot sec^{2} \cdot kg^{-1}$

1.1.9.4.2. $R \approx 2.65 \cdot 10^{5}\ Pa \cdot sec \cdot kg^{-1}$

1.1.9.4.3. $C \approx 3.4 \cdot 10^{-8}\ m^{3} \cdot kg^{-1}$ Note that the capacitance of the lung is a function of its internal volume and that it changes as a function of the differential pressure across the thoracic wall. The algorithm for calculating the current capacitance of the lung is as follows. The capacitance due to volume is calculated and multiplied by a ratio, which is dependent on the transmural pressure across the thorax. The volumetric capacitance is calculated from: $\mathbf{C = \frac{V}{R_G \cdot T}}$. The formula for calculating the ratio of current lung capacitance to that estimated from its volume is:

$$\mathbf{MAX\,(Ratio = MaxRatio + (P_{Lung} - P_{cabin}) \cdot Slope),\, MinRatio)}$$

Where for the human lung :

MaxRatio = 5.0
Slope = $-7.0 \cdot 10^{-3}\ Pa^{-1}$
MinRatio = 1.0

These values were chosen by comparing capacitance calculated purely from volume to those given in the literature for the static pressure-volume diagram for the lung.

1.1.10. Lung Simulator. The values chosen for the Lung Simulator volumes and flow resistance were supplied by Lt. Woods of AL.

1.1.10.1.1. Anatomic Deadspace Volume. $V_D \approx 200\ cm^3$.

1.1.10.1.2. Volume. $V_{LSV} \approx 3{,}500\ cm^3$.

1.1.10.1.3. Total Volume including connecting hose. $V_{LTLC} \approx 3{,}700\ cm^3$.

---

[4] Rahn, H., Otis, A.B., Chadwick, L.E., and Fenn, W.O. The Pressure-Volume Diagram of the Thorax and Lung. Amer. J of Physio. 146(6):161-178. (1946).

1.1.10.1.4. Effective Cross Sectional Area. $A \approx 0.159$ cm^2 (effective diameter ≈ 4.5 mm)

1.1.10.1.5. $L \approx 1.0 \cdot 10^3$ Pa·sec^2·kg^{-1}

1.1.10.1.6. $R \approx 2.0 \cdot 10^7$ Pa·sec·kg^{-1}

1.1.10.1.7. $C \approx 4 \cdot 10^{-8}$ m^3 ·kg^{-1} .

1.1.10.1.8. MaxRatio = MinRatio = $1.0 \cdot 10^{-2}$

1.1.10.1.9. Slope = 0.0

Note that these values were chosen empirically to match the peak pressures measured in the Lung Simulator Experiments.

4.2 Lung Pressure-Volume Relationship. The pressure-volume data of Rahn et al.[1] were digitized. Rahn et al. data represent the average of static pressure-volume measurements taken in three different experiments which enabled the measurement of the pressure-volume relationships of the human thorax in seated men during maximum expiration, maximum inspiration and in the relaxed chest. Rahn et al. used 12 subjects, 11 subjects, and 14 subjects, respectively, for their measurements. It is important to note that Rahn et al. data were taken at during static equilibrium conditions, *i.e.,* no flow conditions. There was considerable variation about the averages. Standard deviations were sometimes as high as 25% of the mean values. Also note that Rahn et al. had to extrapolate their measured data to close the pressure-volume diagram at its extremes because of safety considerations. Nevertheless, Rahn et al.data represent(s) the best data available to the authors for use in this project. Their mean values are shown graphically in Figure 4.2-1, which is usually known as a P-V Diagram. To convert the values on the ordinate to lung volume, one must add the Residual Volume to the indicated percentage of the Vital Capacity.

For the LPT Model, the relevant portions of the P-V diagram are the relaxed chest portions and the portions at the upper right, which relate the lung volume to the higher transmural pressures. Those data are shown graphically in Figure 4.2-2. At the onset of decompression, the most likely scenario would have the aviator in relaxed breathing so that his lung pressure and volume are on the "relaxation pressure curve." If the decompression is rapid enough, a transient transmural pressure will develop across the chest, and the lung volume will move toward the upper part of the relaxation curve where it intersects the maximum inspiratory curve. As the differential pressure rises, the lung volume increases along the maximum inspiratory curve to the upper-right. As the pressure and volume continues to increase a region is reached where lung injury may occur. This is shown as a shaded region on Figure 4.2-2. Note that this limit is not based on measured data, but is generally accepted by the aviation physiology community to be a reasonable limit for safety, although short duration exposures above 100 mmHg have been tolerated in experiments known to this author as the "EONS Experiments." Unfortunately, there were no dynamic pressure-volume tolerance data, nor are there dynamic P-V diagrams available for use in this project.

Figure 4.2-1: Pressure-Volume Diagram for Human Thorax

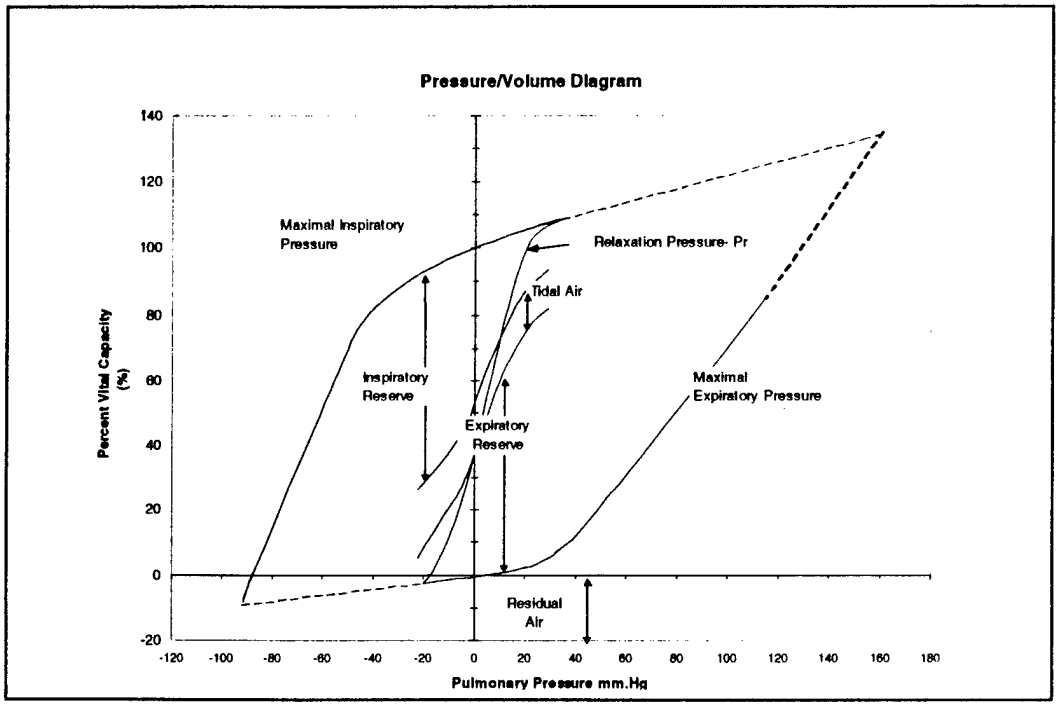

Figure 4.2-2: Pressure-Volume Injury Criterion

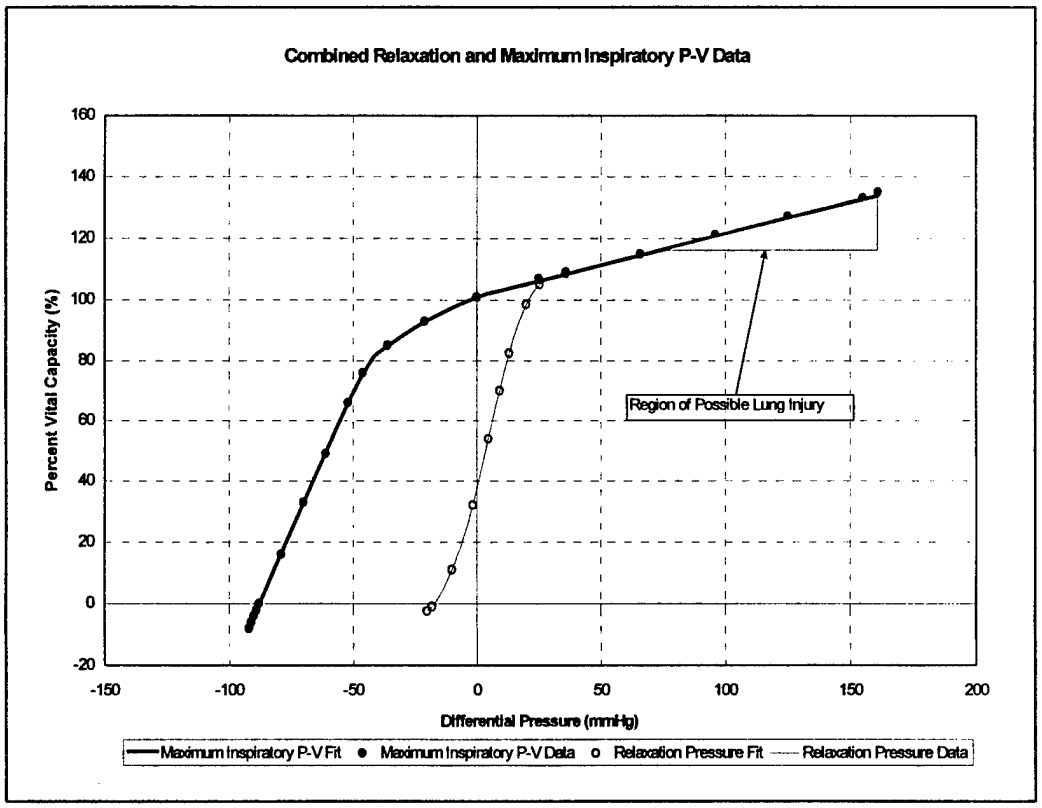

4.3 CRU-73/A Regulator Poppit Valve Pressure-Area Relationship. The performance specification for the regulator outlet poppit valve is controlled by MILSPEC MIL-R-83178, dated 10 Feb 81. The required test performance was employed to estimate the effective area of the valve. This enabled a flow-pressure model to be created using conventional compressible flow models. Figure 4.3-1 shows the area pressure relationship for the poppit valve and Figures 4.3-2 and 4.3-3 illustrate the valve mass and volume flow characteristics at ground level and altitude.

It should be pointed out that the MILSPEC is a manufacturers' performance standard and actual in service regulators may vary somewhat from the minimum standards laid down by the MILSPEC. This is also true of the pressure breathing level supplied by the regulator at altitude.

Figure 4.3-1: Differential Pressure vs Area Characteristics for the CRU-73/A Outlet Relief Valve

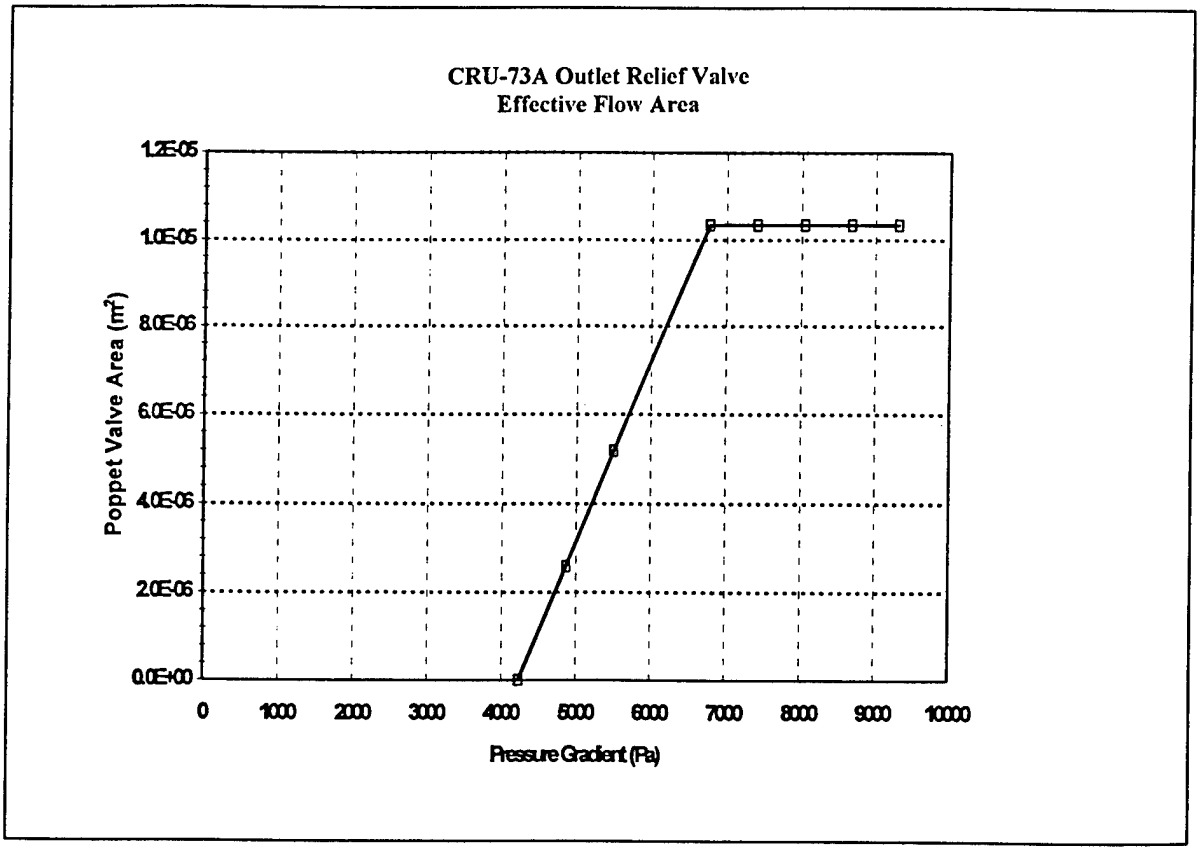

Figure 4.3-2: Regulator Outlet Relief Valve Mass Flow Performance

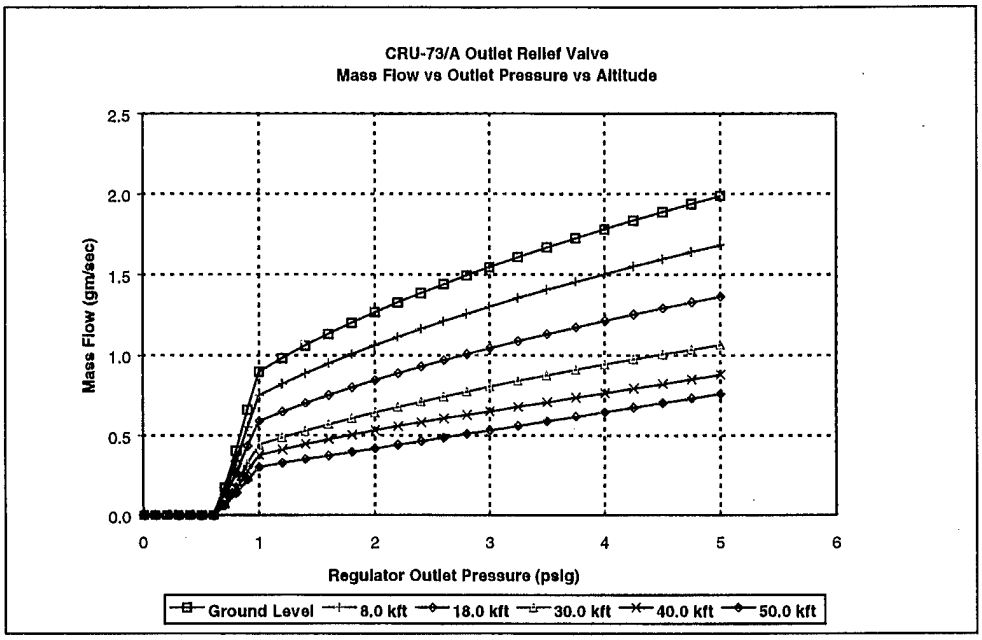

Figure 4.3-3: Regulator Outlet Relief Valve Volume Flow Performance

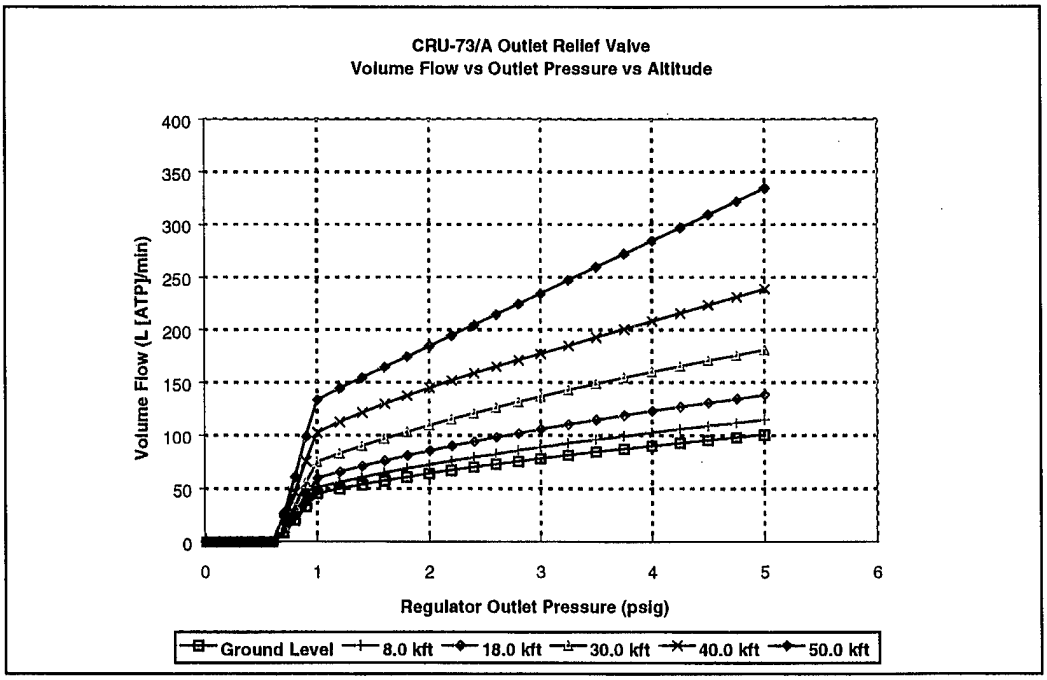

4.4 MBU-12/P Oxygen Mask Expiratory Valve Flow-Pressure Characteristics. The Oxygen Mask incorporated in the MBU-19/P AERP Ensemble is an MBU-12/P. For the LPT Model the flow-pressure characteristics of the expiratory valve were estimated from unpublished laboratory data available to BRC. J. Bomar and R. Holden collected these data in late 1984 at the USAF School of Aerospace Medicine, Crew Systems Branch. The ground level data were employed to characterize the uncompensated performance of the MBU-12/P expiratory valve and to estimate its effective flow area. Figures 4.4-1 and 4.4-2 illustrate the valve's performance at ground level and altitude. Given that the mask cavity absolute pressure is the inlet pressure for the expiratory valve, pressure compensation was accounted for in the model by modeling the pressure in the mask tube and using the mask tube absolute pressure as the valve outlet pressure.

Figure 4.4-1: Differential Pressure vs. Area Characteristics for the MBU-12/P Expiratory Valve

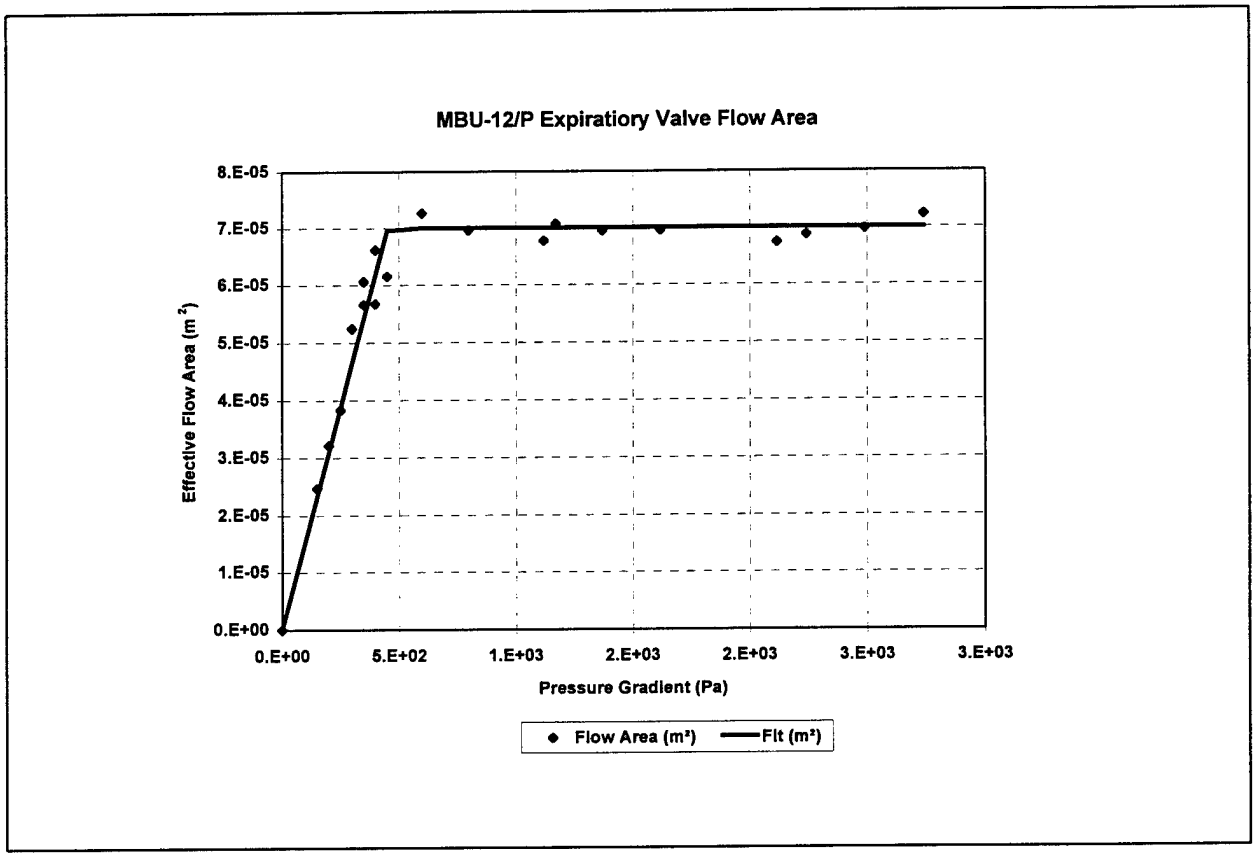

Figure 4.4-2: MBU-12/P Expiratory Valve Flow Characteristics

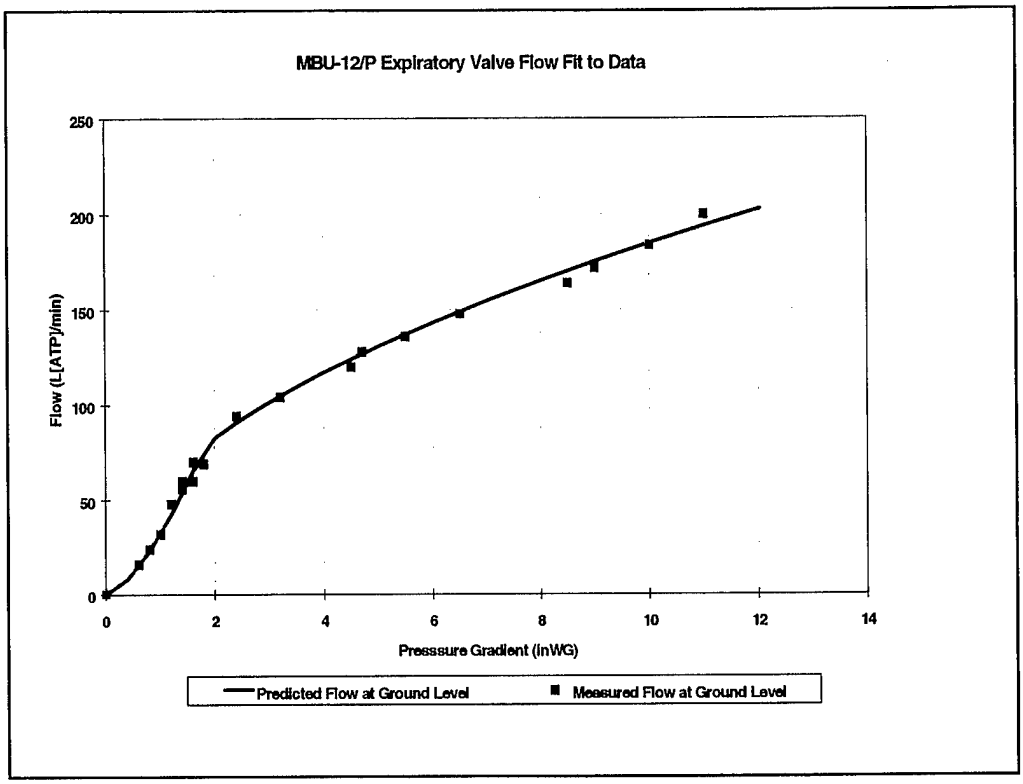

Figure 4.4-3: MBU-12/P Expiratory Valve Volume Flow Characteristics

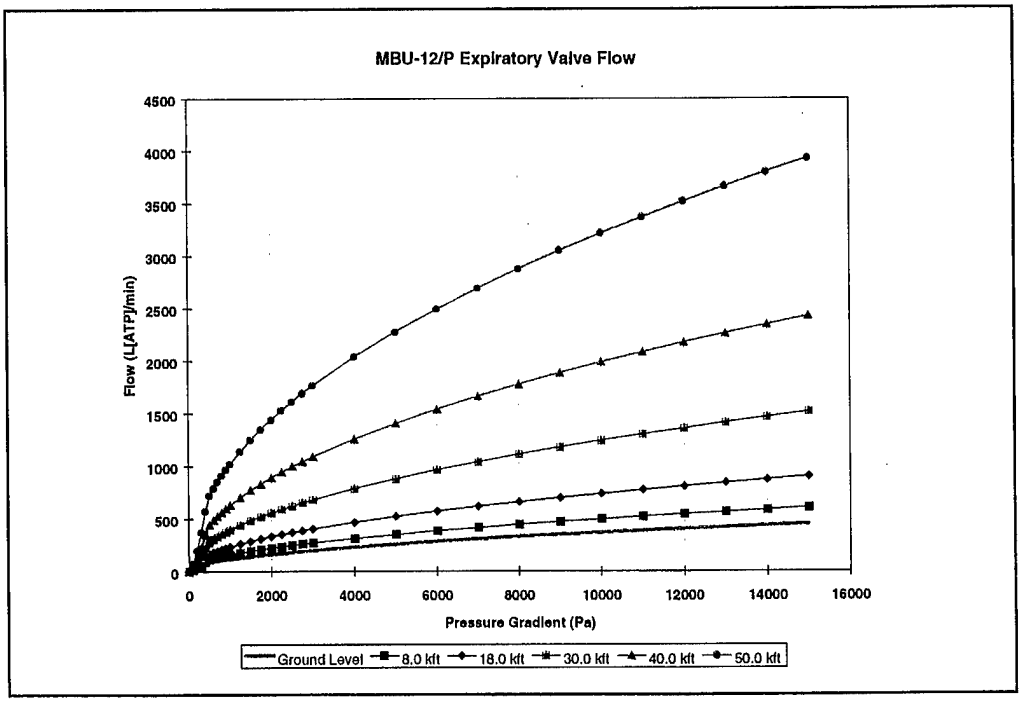

5.0 Source Code Listings. A copy of the executable computer program has been delivered to the Air Force. The source code listings of the Fortran Model sections of the program are included to aid in understanding the operation of the program. The source code is copyrighted by Biodynamic Research Corporation and may not be copied or distributed outside the US Government. All rights to this code are retained by BRC except for use of the executable version by the US Government.

5.1 Fortran Code which Defines the Differential Equations for the Integrator.

```
! LPTModel.f90     COPYRIGHT BIODYNAMIC RESEARCH CORP 1997 SAN ANTONIO TEXAS ! !USA
! 'Unauthorized copying or distribution of this software
! outside the U.S. Government is prohibited.
! The CONTAINED SUBROUTINE RES contains the dynamics and kinematics of the Lung Pressure Transient
! system.  It forms the differential equation residuals expected
! by DDASSL.
!
! The subroutine has the call parameters required by the original DDASSL
! numerical integrator.
!
SUBROUTINE RES(Tdummy, Ydummy, YPdummy, DELTA, IRES, RPAR, IPAR)
 USE Precision_Defs
 USE Global_Variables
 USE Pneumatics
!
! Details of differential equations describing the dynamics of
! The Lung Pressure Transient (LPT) Model 5/23/97
! J. Bomar, Biodynamic Research Corporation, 9901 IH-10W, Ste 1000, San Antonio, TX 78230
! All rights reserved.
!
!  NOTE: The subscript notation indicates the derivative WRT the
!       subscript  E.G.  Xt ==> The first derivative of X
!       WRT time.
!
!  The LPT Model estimates the time history of pressures in the Lung and in the relevant portions
!  of an aviator's breathing system during a decompression of the pressure cabin of an aircraft.
!  For this initial version of the model the modeled system is specifically and exclusively the MBU-19/P
!  NBC protective system also known as the Aircrew Eye Respiratory System (AERP).  The AERP comprises an
!  MBU-12/P oronasal mask installed in a chemically protective hood designed to envelop the head. The
!  inspiratory flow path is protected by a charcoal/particulate filter cannister installed in the hose
!  between the regulator outlet and the mask tube inlet.  The LPT Model includes only those components of
!  CRU-73/A - AERP system that are relevant to a decompression, ie the regulator's normal function is not
!  modeled. The components included in the model are:
!
!     1.  CRU-73/A Diluter-Demand Breathing Regulator.  The outlet relief valve is characterized as a
!         variable area orifice whose area is a function of the differential pressure between the
!         regulator outlet and the cabin ambient.  The volume of gas in the regulator outlet compartment
!         is included.
!         a) Outlet Volume.  VRO » 45 cm3 = 2.75 in3 (Estimate provided by Mr. Chrome).
!         b) Cracking Pressure.  PRVCP » 17 inH2O = 31.8 mmHg
!         c) Full Open Pressure.  PRVFO » 0.98 psig =  50.8 mmHg
!         d) Flow when fully open QFO » 45 L·min-1 @ NTPD
!         e) Effective Area.  ARV approx  0.11 cm2.
!     2.  Regulator Outlet Hose.  These values are estimates and are likely to vary with the configuration of
!         the regulator installation.  The USAF is to provide the final values for the model.
!         a) Length.  IRH » 36 in = 0.91 m
!         b) Effective Diameter.  dRH » 0.75 in  = 1.9 cm
!         c) Volume.  VRH » 0.26 L = 2.6 · 10-4 m3
!         d) Flow Resistance.  A quadratic flow pressure relationship was estimated from theoretical
!            flow-pressure models.  The model employed is DP = 1.74·104 Q + 2.62·107 Q2 .  Where, DP is given
!            in Pascals and Q is given in meters3·sec-1.
!     3.  Canister Pigtail Adapter.  These values are estimates.  The final values are to be supplied by the
!         USAF.
!         a) Length.  ICP » 6 in = 15 cm
```

! b) Effective Diameter. dCP » 0.75 in = 1.9 cm
! c) Flow Resistance. A quadratic flow pressure relationship was estimated from theoretical
! flow-pressure models. The model employed is DP = 1.74·104 Q + 2.62·107 Q2 . Where,
! DP is given in Pascals and Q is given in meters3·sec-1.
! 4. Canister. These values were supplied by Racal to Lt. Woods.
! a) Volume. VCT » Total = 4.91 cm3 = 80.5 cm3, Charcoal Volume = 2.14 in3 = 35 cm3, and Void
! Volume, VCV = 2.77 in3 = 45.5 cm3.
! b) Flow Resistance. RC approx = 5. x 10-2 mmHg·L-1·min NTPD (linear). (This is equivalent to
! approximately 5.4 inWG at 200 L-1·min-1 NTP D or 666 Pa at 3.33·10-3 m3·sec-1)
! 5. MBU-19/P Manifold. These values are estimates. The final values are to be supplied by the USAF.
! a) Volume. VCM approx = 40 cm3.(per measurements at BAFB)
! b) Flow Resistance. RC approx = 1.0 x 10-2 mmHg·L-1·min-1 NTP D (linear).
! (This is equivalent to approximately 1 inWG at 200 L-1·min-1 NTP D or 249 Pa at 3.33·10-3
! m3·sec-1.)
! 6. Mask Tube. Gentex West supplied the value for volume.
! a) Volume. VMT approx = 174 cm3.
! b) Diameter. dMT approx = 0.75 in = 1.9 cm. Implies 24in length = 61 cm
! c) Flow Resistance. A quadratic fit to unpublished laboratory data was employed to create the
! following flow vs pressure loss model. DP = 7.5·103 Q + 4.5·106 Q2 . Where, DP is given in
! Pascals and Q is given in meters3·sec-1.
! 7. Oxygen Mask. Gentex West supplied the values for volume and flow resistance. Additional flow
! resistance data were taken from unpublished laboratory data available to Dr. J. Bomar.
! a) Mask Deadspace. VM approx = 230 cm3
! b) Expiratory Valve Flow Resistance.
! (1) Cracking Pressure. PMXVCP = 0.0 Pa
! (2) Maximum Area. AMMXV = 7.0·10-5 m2.
! (3) Pressure required to reach AMMXV. PMMXV = 450 Pa
! c) Mask Leakage. (These are estimated values).
! (1) Maximum Sealing Pressure. PMLSM approx = 4000 Pa
! (2) Seal Failure Pressure. PMLSF approx = 8000 Pa
! (3) Flow with seal failed. QMLSF = 1.67 m3·sec-1
! d) Expiratory Valve Shroud. These values are estimates. The final values are to be supplied by the
! USAF.
! e) Effective Volume. VEVS approx = 198 cm3 (per measurements at BAFB)
! f) Flow Resistance of Shroud Vents.
! (1)
! 8. NBC Hood. These values are estimates. The final values are to be supplied by the USAF.
! a) Effective Volume with Helmet. VH approx 1 liter .
! b) Relief Valve Cracking Pressure. DPHRVCP = 0.1 inWG.
! c) Relief Valve Flow Resistance. DPHRV(, ARV, CD) = 0.1 inWG at 20 L-1·min-1 NTP D1. (per estimate
! by Mr. J. Damron, ILC Dover)
! 9. Pulmonary System. The values chosen for lung volumes and flow resistance were determined from
! published references as given below.
! a) Anatomic Deadspace Volume. VD approx = 150 cm3
! b) Lung Volume (End Inspiratory Volume). VLEIV approx = 3,000 cm3.
! c) Vital Capacity VLVC approx = 4,500 cm3.
! d) Residual Volume. VLRV approx = 1,500 cm3.
! e) Total Lung Capacity. VLTLC approx = 6,000 cm3.
! f) Effective Cross Sectional Area of Trachea. AT approx = 0.2 cm2 (effective diameter
! approx = 5 mm)
! g) Flow Resistance of Upper Airways. The upper airway flow resistance will be approximated using a
! "lumped parameter model" by employing an orifice model using the area dimensions given above.
! Distributed resistance models are available e.g. see Weibel . However, such models are
! computationally complex and the lumped parameter model will be employed unless it is determined
! that the internal flow resistance of the lung contributes significantly to transmural pressure
! developed across the thorax during RD.
! h) Chest Wall. For the purposes of setting the upper allowable limit for hazardous lung/chest
! expansion, the static P-V diagram will be employed. Rahn, et al , gave an example of such a P-V
! diagram.
! i) Diaphragm. The compliance of the diaphragm will be lumped with the chest wall compliance unless
! it is found necessary to model the diaphragm's compliance separately.
! j) Dynamic Expansion of the Thorax. The model of Mead and Milic-Emili1 will be employed. Their
! model is a second order lumped parameter model of the form,
! dP/dt = Ld^2Q/dt^2 + RdQ/dt + (1/C)Q
! Where, P is differential pressure, Q is volume, R is flow resistance, L is flow inertance,
! and C is capacitance.
! (1) L approx = 1.2·10^2 Pa·sec^2·kg^-1

```
!          (2) R approx = 2.65·105 Pa·sec·kg^-1
!          (3) C =  Max(MaxRatio+(Plung – Pcabin)*Slope, MinRatio)* Vlung/(Rg*T)
!                   MaxRatio = 5, Slope = -7*10^-3 Pa^-1, MinRatio = 1.0
!        !
!  Lung Pressure Model
!
!    The time rate of change of mass in the lung is given by
!
!          d(Vl·Pl)/dt = rhoin·Qin - rhoout·Qout
!
!          Pl dVl/dt + Vl dPl/dt = rhoin·Qin - rhoout·Qout
!
!          In a decompression, Qin = 0, therefore
!
!          dPl/dt = Pl/Vl·(Qout - dVl/dt),
!
!         Where, Qout is a function of the quantity of flow through the trachea into the
!         mask and (normally) then out through the expiratory valve and shroud, and Vl and Pl are the
!         Volume and Pressure in the lung, rho is density and the Q's are volumetric
!         flows in and out of the trachea.
!
!        Note that rho = Pabs/(Rgas·Tabs)
!           Pabs   = Absolute Pressure [Pa]
!           Rgas   = Specific gas constant Runiv/MWgas [N·m/(kgmol·K)]
!           Tabs   = Temperature in deg K
!
!          So that, rholung = Plung/(Rgas*Tbody)
!           Where,
!                Rgas = Runiv/MW pulmonary gas
!
!          Molecular Wt calculated as follows
!        Ptot FO2   FCO2  Finert  FH2O  MWGas
!         760 0.137 0.050 0.751  0.062 28.73
!         570 0.182 0.067 0.668  0.082 28.97
!         380 0.274 0.100 0.503  0.124 29.46
!
!         So use MWAir as the Nominal MW of the breathing gas in the LPT Model
!
!          In the case of of a rapid decompression as the ambient pressure in the cabin falls, gas must
!          flow from the lung outward to equalize the lung's internal pressure with that of the ambient.
!          The normal path for outward flow is through the oronasal mask expiratory valve. In the case of
!          significant mask leakage into the hood envelope, the gas must pass out through the hood relief
!          valve.  The Mask Expiratory Valve backpressure is a function of its compensation pressure which
!          is set by the pressure in the mask tube.  That pressure is set by the regulator outlet
!          pressure. In a decompression, the regulator outlet pressure remains constant at the pre-
!          decompression pressure until the ambient pressure falls approximately 1 psig below the
!          pre-decompression pressure at which time the regulator's outlet relief valve opens allowing
!          the contents of the inspiratory path to vent in a retrograde flow out through the regulator's
!          outlet chamber to ambient.  As the regulator outlet pressure falls, the compensation of the
!          Mask expiratory valve is reduced allowing it to open and release the gas from the trachea and
!          lung.
!
!      Set Up Differential Equations
!
!  Ydummy(1) [=] Cabin Pressure
!  Ydummy(2) [=] Lung Pressure
!  Ydummy(3) [=] Lung Volume
!  Ydummy(4) [=] First Derivative of Lung Volume
!  Ydummy(5) [=] Mask Pressure
!  Ydummy(6) [=] Regulator Outlet Pressure
!  Ydummy(7) [=] Mask Tube Pressure
!  Ydummy(8) [=] Mask Tube Volume
!  Ydummy(9) [=] First Derivative of Mask Tube Volume
! Ydummy(10) [=] Hood Pressure

!
 IMPLICIT NONE
```

```
  REAL(LongR), INTENT(INOUT) :: Tdummy
  REAL(LongR), INTENT(IN), DIMENSION(NEQ) :: Ydummy, YPdummy
  REAL(LongR), INTENT(OUT), DIMENSION(NEQ) :: DELTA
  INTEGER(LongI), INTENT(INOUT) :: IRES(1)
  REAL(LongR), INTENT(IN) :: RPAR(1)
  INTEGER(LongI), INTENT(IN) :: IPAR(1)
  REAL(LongR), DIMENSION(NEQ) :: Yderiv
  REAL(LongR) :: MaskValveDiff, InspValveArea = 1.5D-4, &
            InspValveVolFlow, InspValveMassFlow, InspValveDiffP, CapRatio
  INTEGER(LongI) :: i ! index variable
!
!
! Calculate the Flow out of the Regulator Poppit Valve and Mask ExValve
!
!    SUBROUTINE Orifice_Flow(CDorifice, Area, P_upstream, P_downstream, &
!    T_absolute, Molecular_Weight, Volume_Flow, Mass_Flow, P_critical)
!
! Aflow =MIN(MAX(0.0D0,icept + slope*Pout), Amax)
!
!
    CabinPressure = DMAX1(Ydummy(1), AmbientPressure)
!
! To approximate the cabin temperature change during the decompression
! use the polytropic coefficient 1.2 which lies between adiabatic and isothermal
! decompressions. Then Tcabin/TcabinInitTemp = (CabinTemp/CabinInitTemp)^((k-1)/k)
!
    CabinTemp = (CabinPressure/CabinInitPressure)**km1ok * CabinInitTemp
!
! Calculate the PBA pressure for the CRU73. PBforA returns ATA so convert to Pa.
!
    PBAPressure = PBforA(CabinPressure/Pstandard)*Pstandard
!
! Regulator outlet differential WRT cabin
!
    RegOutDiffP = DMAX1(CabinPressure, (Ydummy(6) + PBAPressure)) - CabinPressure  ! RegOutAbsP - AmbientAbsP
!
! Compute Flow Area for Regulator Relief Poppit
!
    RegPoppitArea = DMIN1(DMAX1(0.0D0, IceptdAdPRegPoppit + &
    SlopedAdPRegPoppit*RegOutDiffP),  Regulators(1)%ReliefPoppit%MaxArea) + 1.0D-7 ! Add small
!                                                    ! Leakage Area
! Compute Regulator relief valve flow
!
    CALL Orifice_Flow( 1.0D0, RegPoppitArea, DMAX1(CabinPressure, Ydummy(6)+PBAPressure), &
    Ydummy(1), CabinTemp, MWAir, RegPoppitVolFlow, RegPoppitMassFlow, P_Crit)
    RegPoppitVolFlow = DMAX1(RegPoppitVolFlow,  0.0D0)  ! One Way Valve but can leak at 0.2 L/m
    RegPoppitMassFlow = DMAX1(RegPoppitMassFlow, 0.0D0)

!
! Mask differential WRT cabin
!
    MaskTubeAbsP = Ydummy(7)
    MaskDiffP = Ydummy(5) - CabinPressure !  Mask Cavity Pabs - Regulator Outlet Pressure
    MaskValveDiff = Ydummy(5) - (MaskTubeAbsP - 100.d0)
! Subtract 1 inWG from compensation pressure to account for its inefficiency

!
! Compute Flow Area for Mask Exp Valve
!
    MaskExValveArea = DMIN1(DMAX1(0.0D0, IceptdAdPMaskExValve + &
    SlopedAdPMaskExValve*MaskValveDiff), Masks(1)%ExValve%MaxArea)
!
! Compute Mask Ex Valve flow
!
    CALL Orifice_Flow( 0.68d0, MaskExValveArea, Ydummy(5), MaskTubeAbsP-100.D0, &
    Masks(1)%MaskTemp, MWAir, MaskExValveVolFlow, MaskExValveMassFlow, P_Crit )
    MaskExValveVolFlow = DMAX1(MaskExValveVolFlow,  0.0d0)  ! One Way Valve
```

```
    MaskExValveMassFlow = DMAX1( MaskExValveMassFlow, 0.0d0)
!
! Compute Mask Insp Valve flow
!
!
    IF ( MaskTubeAbsP > Ydummy(5)+100.D0 ) THEN   ! add 1/2 inWG bias to keep mask insp valve closed
                                                  ! at very low pressure difference
      CALL Orifice_Flow(0.68D0, InspValveArea, MaskTubeAbsP, Ydummy(5)+100.D0,  &
      Masks(1)%MaskTemp, MWAir, InspValveVolFlow, InspValveMassFlow, P_Crit )
     ELSE
      InspValveVolFlow  = 0.0D0
      InspValveMassFlow  = 0.0D0
    END IF
    InspValveVolFlow = DMAX1(InspValveVolFlow,  0.0d0)  ! One Way Valve
    InspValveMassFlow = DMAX1(InspValveMassFlow, 0.0d0)
!
! Hood differential WRT cabin
!
    HoodDiffP = Ydummy(10) - CabinPressure
!
! Compute Area of Hood Poppit
!
    HoodPoppitArea = DMIN1(DMAX1(0.0D0, IceptdAdPHoodPoppit + &
    SlopedAdPHoodPoppit*HoodDiffP),  Hoods(1)%ReliefValve%MaxArea)
!
! Compute Hood Relief Valve flow
!
    CALL Orifice_Flow( 0.68d0, HoodPoppitArea, Ydummy(10), &
    Ydummy(1), CabinTemp, MWAir, HoodReliefValveVolFlow, HoodReliefValveMassFlow , P_Crit)
    HoodReliefValveVolFlow = DMAX1(HoodReliefValveVolFlow,  0.0d0)  ! One Way Valve
    HoodReliefValveMassFlow = DMAX1(HoodReliefValveMassFlow, 0.0d0)
!
! Trachael area is a constant in this model
!
    TracheaDiffP = Ydummy(2) - Ydummy(5) !  LungPabs - MaskPabs
    CALL Orifice_Flow( 1.0d0, TrachealArea, Ydummy(2), Ydummy(5), &
    BodyTemp, MWAir, TrachVolFlow, TrachMassFlow,  P_Crit )

    LungDiffP = Ydummy(2) - CabinPressure   ! Lung Pabs - Cabin Pabs

!
! Mask Tube Flow Calculation-- Inspiratory path resistance is represented by a fixed
! Equivalent Orifice in this model
!
    MaskTubeDiffP = MaskTubeAbsP - CabinPressure  !  Compensation Pressure
    CALL Orifice_Flow( 0.68d0, Connectors(1)%EffCrossSecArea, MaskTubeAbsP,  &
    Ydummy(6)+PBAPressure, CabinTemp, MWAir, MaskTubeVolFlow, MaskTubeMassFlow,  P_Crit )
!
! Set up system of DAE equations
!
!   YPdummy(1) [=] Rate of Change in Cabin Pressure
!   YPdummy(2) [=] Rate of change in Lung Pressure
!   YPdummy(3) [=] Rate of change Lung Volume
!   YPdummy(4) [=] Second Derivative of Lung Volume
!   YPdummy(5) [=] Rate of change Mask Pressure
!   YPdummy(6) [=] Rate of change Regulator Outlet Pressure
!   YPdummy(7) [=] Rate of change Mask Tube Pressure
!   YPdummy(8) [=] Rate of change in Mask Tube Volume
!   YPdummy(9) [=] Second Derivative of Mask Tube Volume
!  YPdummy(10) [=] Rate of change Hood Pressure
!
!  Set up Cabin Pressure Diffeq [=] YPdummy(1)
!
! SUBROUTINE Decompression_Rate( CabinVolume, Area_of_Defect, Initial_Cabin_Pressure, &
!    Current_Cabin_Pressure, Ambient_Pressure, Cabin_Temperature, Rate_of_Decompression )
!
! NOTE:  This call defines the rate of change in cabin pressure
```

```
!
    CALL Decompression_Rate(CabinVolume, DefectArea, CabinInitPressure, CabinPressure, &
       AmbientPressure, CabinTemp, Yderiv(1)) ! Defines Rate of change in CabinP
!
!   Rate of change in Lung Pressure
!
!  dPL/dt = -PL/VL*(QtrachOut + dVL/dt)
!
    LungVolume = Ydummy(3) + Lungs(1)%FunctionalResidualVolume
    Yderiv(2) = -Ydummy(2)/LungVolume*(TrachVolFlow  + Ydummy(4))
!
!  Lung Volume Dynamics model accountes for dynamic variation in lung volume
!
!  Yderiv(3) = dVL/dt = Ydummy(4)
!  Yderiv(4) = dVL^2/dt^2 = dVL^2/dt^2 = 1/L*(PL - R*dV/dt - 1/C*VL)
    CapRatio = DMAX1(Lungs(1)%MaxCapRatio + Lungs(1)%SlopeCapRatio*LungDiffP, Lungs(1)%MinCapRatio)

    LungCapacitance = LungVolume/(Rgas*BodyTemp) * CapRatio

    LungGasDensity = Ydummy(2)/(Rgas*BodyTemp)
    Yderiv(3) = Ydummy(4)
    Yderiv(4) = 1.0d0/Lungs(1)%L*(LungDiffP/LungGasDensity - Lungs(1)%R*Ydummy(4) - &
          1.0d0/LungCapacitance * Ydummy(3))
!
!   Mask Pressure dynamics
!
!  dPmask/dt = Pmask/(Vmask*Rgas*Tmask)*(Qtrachvol - Qexpvalve)
!
    MaskDiffP = Ydummy(5) - Ydummy(1)
    IF (MaskDiffP <  Masks(1)%MaxSealP) THEN
       MaskLeakFlow = 0.0D0
     ELSE IF( MaskDiffP > Masks(1)%SealFailP ) THEN
       MaskLeakFlow =  Masks(1)%SealFailFullVolFlow
     ELSE
       MaskLeakFlow = Masks(1)%SealFailInitVolFlow +  &
       (Masks(1)%SealFailFullVolFlow -  Masks(1)%SealFailInitVolFlow)* &
       (MaskDiffP - Masks(1)%MaxSealP) / ( Masks(1)%SealFailP -  Masks(1)%MaxSealP)
    END IF

    Yderiv(5) = Masks(1)%MaskTemp / EffectiveMaskDeadspace * &
          ( Ydummy(2)*TrachVolFlow/BodyTemp + Ydummy(5)*(InspValveVolFlow - &
          MaskExValveVolFlow - MaskLeakFlow)/Masks(1)%MaskTemp)
!
!   Regulator Outlet Pressure dynamics
!

    Yderiv(6) = (Ydummy(6)+PBAPressure) / Volume_Inspiratory_Path  * &
                (MaskTubeVolFlow - RegPoppitVolFlow)

!               Add a small amount of capacitance to the reg outlet hose
!
!  Mask tube pressure dynamics
!
    MaskTubeVol = Masks(1)%MaskTube%Volume + Ydummy(8)
    Yderiv(7) = -MaskTubeAbsP/MaskTubeVol * (MaskTubeVolFlow + InspValveVolFlow + Ydummy(9))

!   Mask tube volume dynamics deltas from basic mask tube volume
    MaskGasDensity = Ydummy(7)/(CabinTemp*Rgas)
    MaskTubeDiffP = Ydummy(7) - Ydummy(1)
    Yderiv(8) =  Ydummy(9)
    Yderiv(9) =  1.0D0/Masks(1)%MaskTube%Inductance * &
          (MaskTubeDiffP/MaskGasDensity - &      ! Mask tube pressure
          Masks(1)%MaskTube%Resistance*Ydummy(9) - &    ! Mask Tube Resistance
          1.0D0/Masks(1)%MaskTube%Capacitance * Ydummy(8))  ! Mask Tube Capacitance
!
!  Hood Pressure dynamics
```

```
!
    Yderiv(10) = Ydummy(10)/Hoods(1)%Volume * (MaskLeakFlow - HoodReliefValveVolFlow)
    DO i = 1, NEQ
      DELTA(i) = Yderiv(i) - YPdummy(i)
    END DO
    tsave = Tdummy
END SUBROUTINE RES
```

REFERENCES

[1] Rahn, H, Otis, AB, Chadwick, LE, and Fenn WO. The Pressure-Volume Diagram of the Thorax and Lung. Am J Physiol 146:161-178, 1946.

[2] Ernsting, J. Physiological Requirements for Advanced Oxygen Systems. In Advanced Oxygen Systems for Aircraft. AGARDOGRAPH 286. North Atlantic Treaty Organization. Neuilly-Sur-Seine, FR. AGARD-AG-286:25, 1996.

[3] Bomar, JB, Scott, MW, and Smith DA. Modeling Respiratory Gas Dynamics in the Aviator's Breathing System. AL/CF-TR-1994-0047. Armstrong Laboratory (AFMC), Brooks AFB, TX, 1994.

[4] Meade, J. Milic-Emili, J. Theory and methodology in respiratory mechanics with glossary of symbols. T Handbook of Physiology, Respiration IV. Chapter 11:363-376. (1981).

[5] Ernsting, J. Cabin Pressurisation Schedules - Acceptable Compromises. In Raising The Operational Ceiling. A WORKSHOP ON THE LIFE SUPPORT AND PHYSIOLOGICAL ISSUES OF FLIGHT AT 60,000 FEET AND ABOVE. Proceedings of a meeting held at Armstrong Laboratory, Brooks AFB, TX, 1995.

[6] Krebs, M.B. Human Pulmonary Tolerance to Dynamic Over-Pressure. USAF Armstrong Laboratory AL/CF-TR-1996-0058. Brooks AFB, TX 78235. (1996).

APPENDIX A:
Gentex Drawings

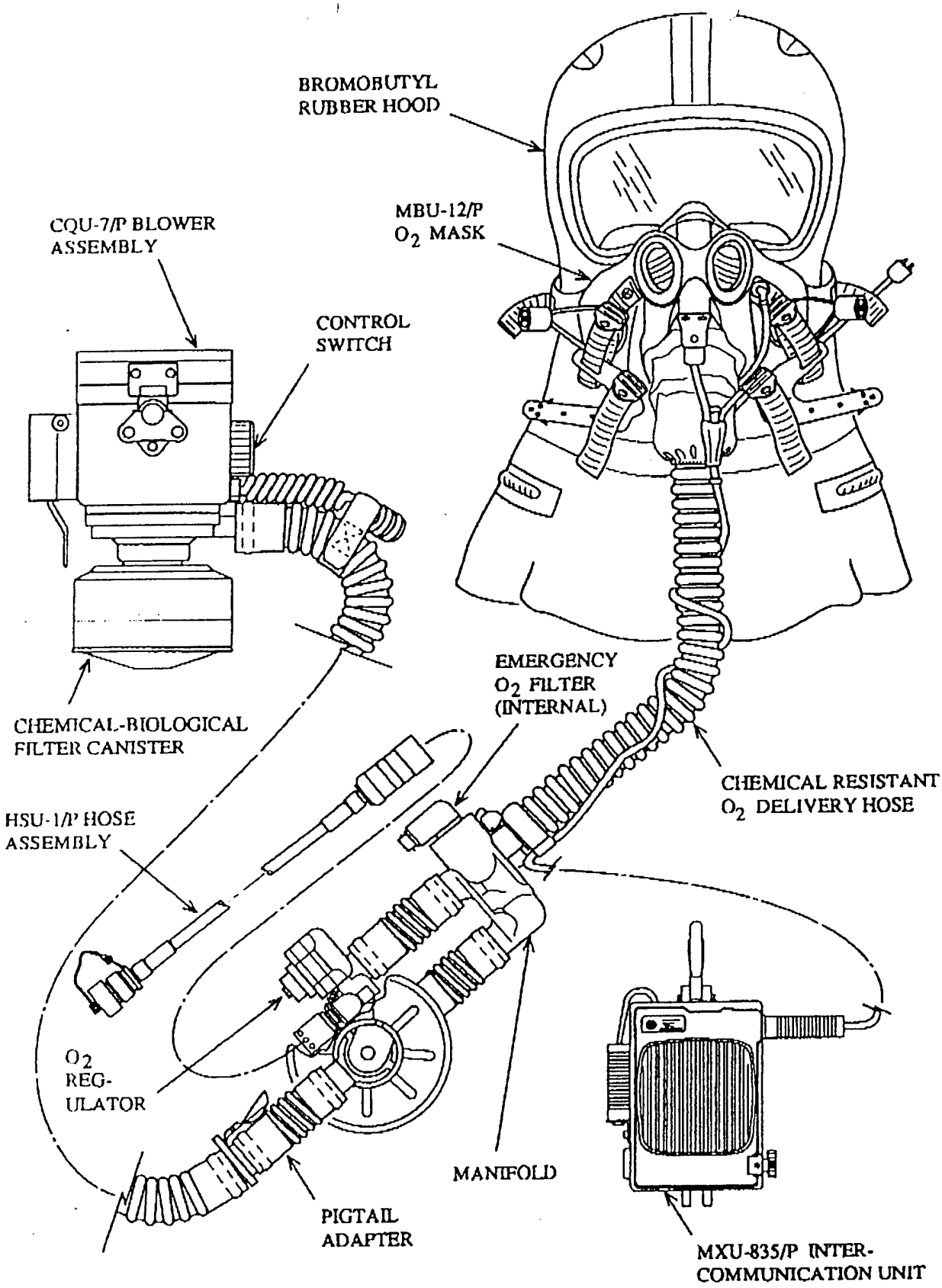

Figure 1-1. MBU-18/P Functional Layout

NOTE: HELMET NOT SHOWN.

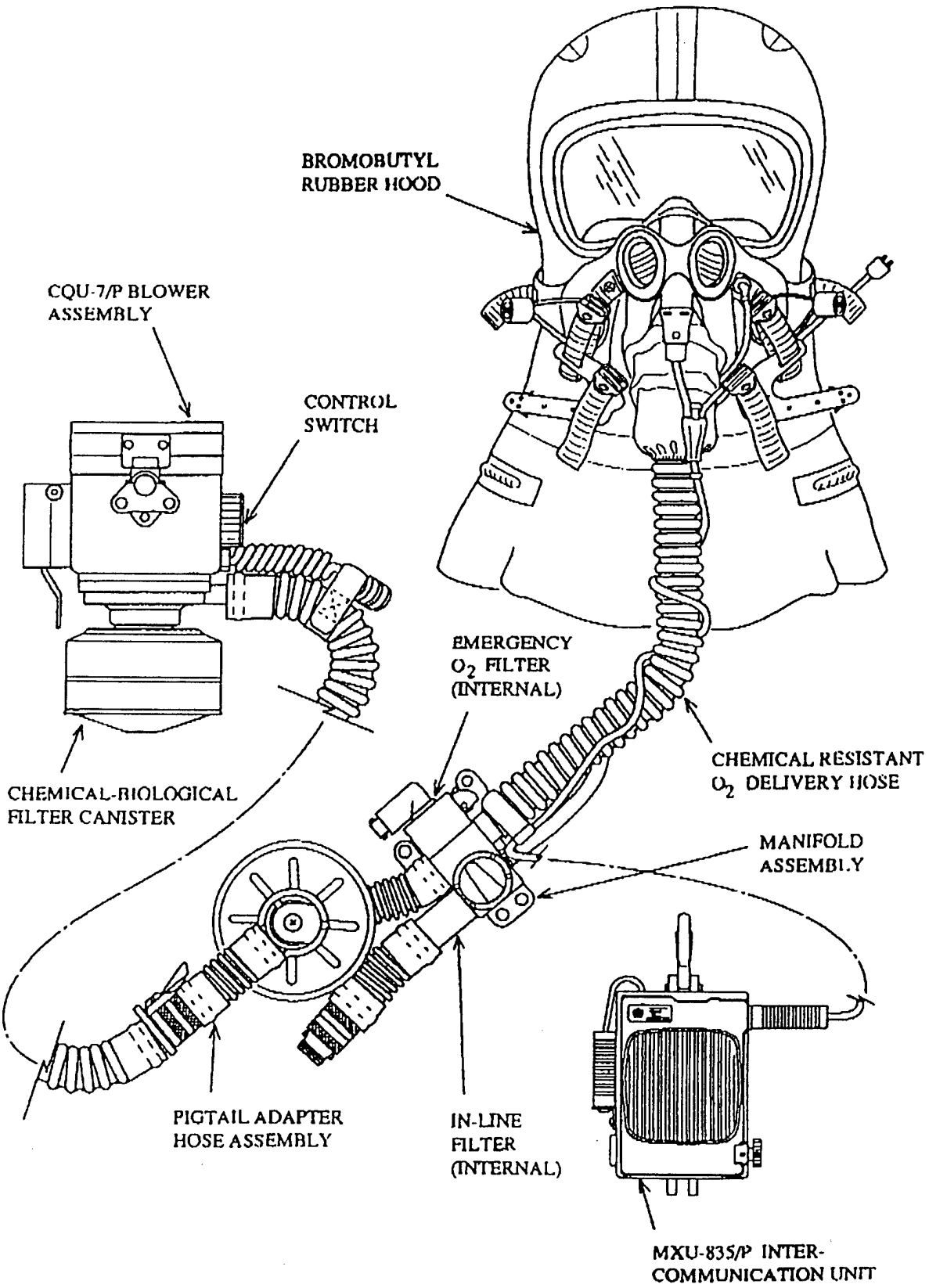

Figure 1-2. MBU-19/P Functional Layout Helmeted Version.

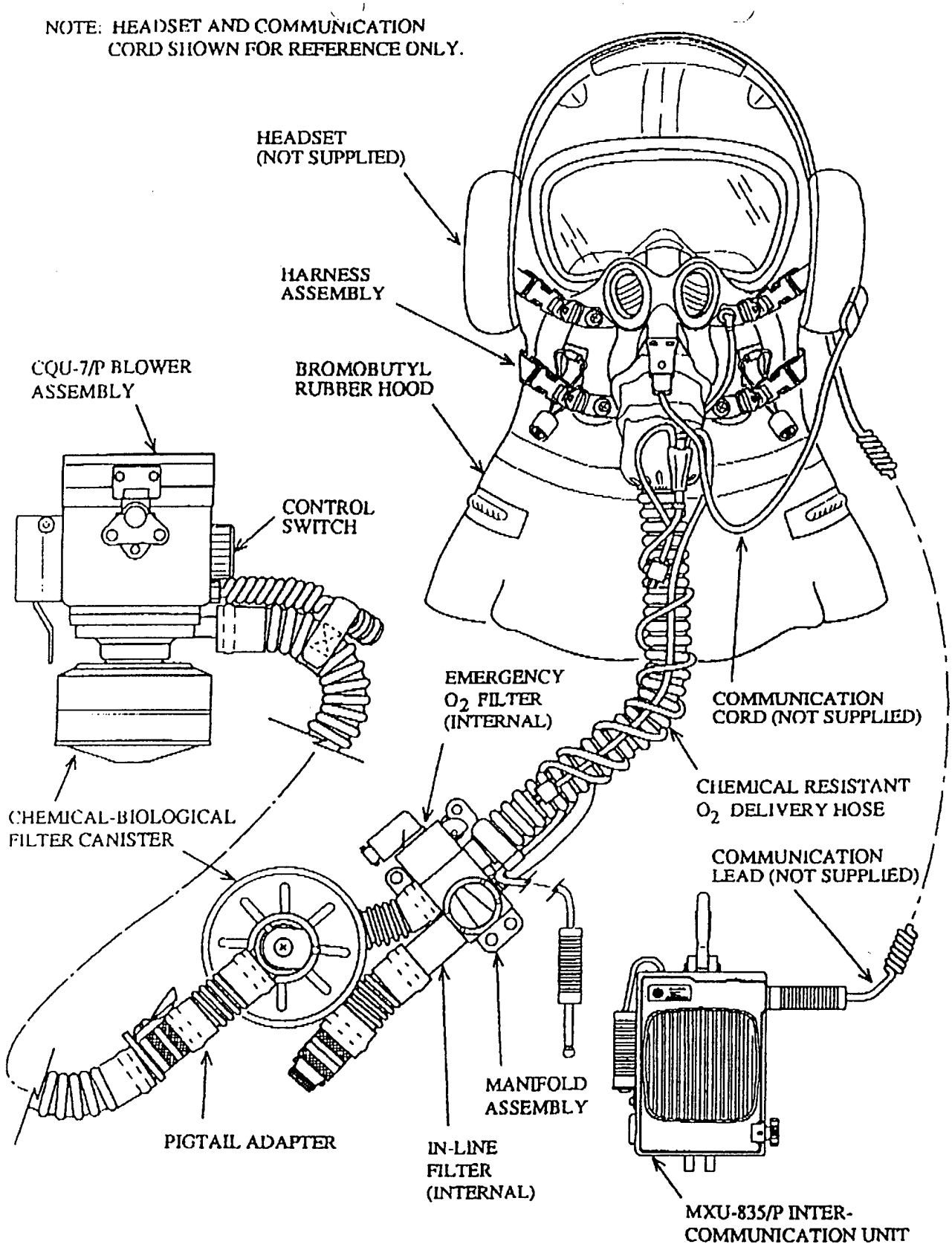

Figure 1-3. MBU-19/P Functional Layout Non-Helmeted Version.

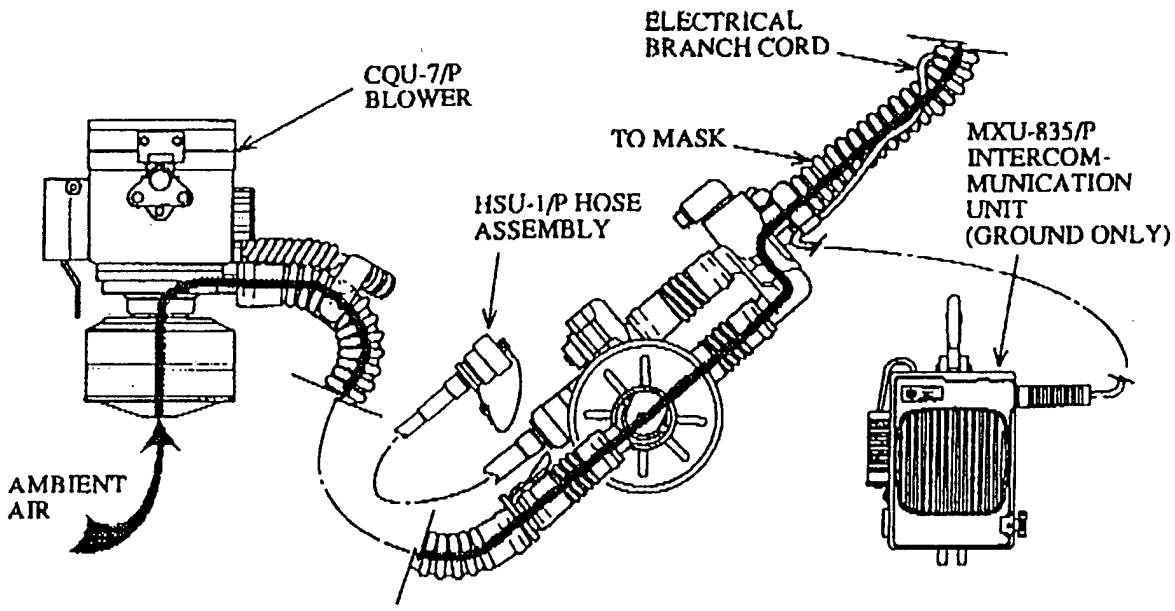

MBU-18/P GROUND OPERATING MODE.

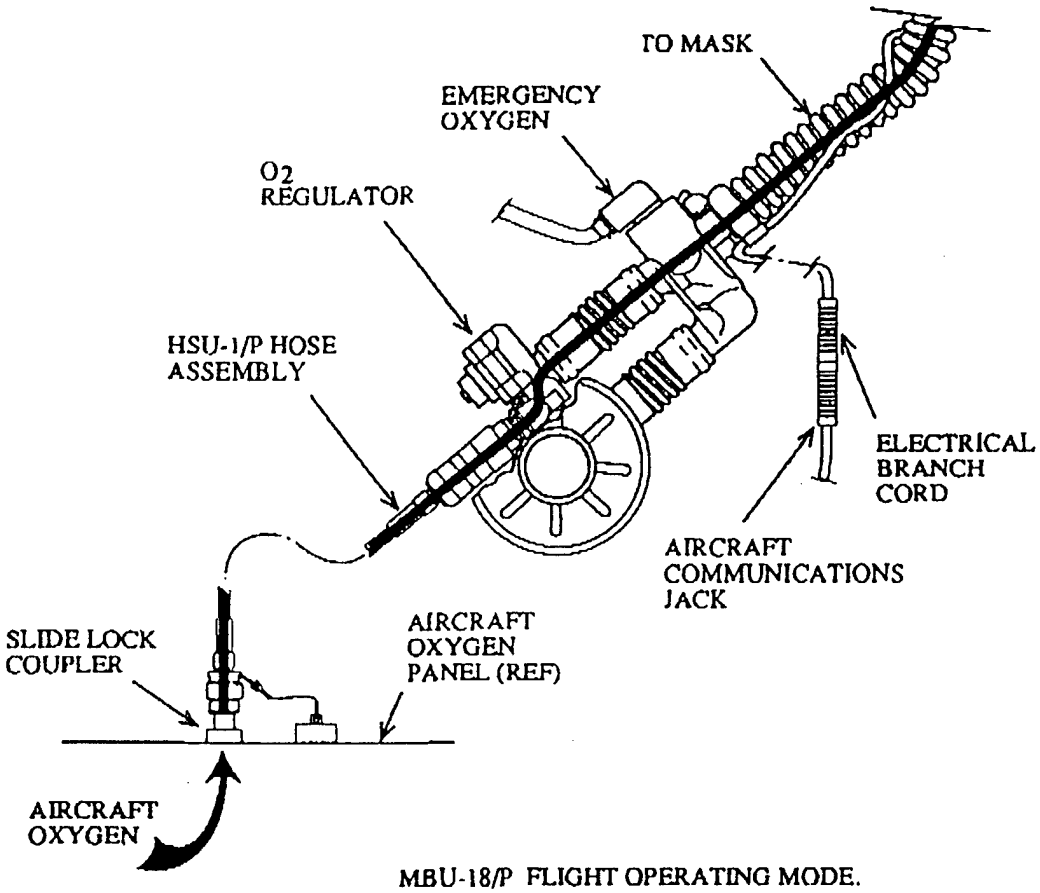

MBU-18/P FLIGHT OPERATING MODE.

Figure 4-1. MBU-18/P Functional Layout.

4-

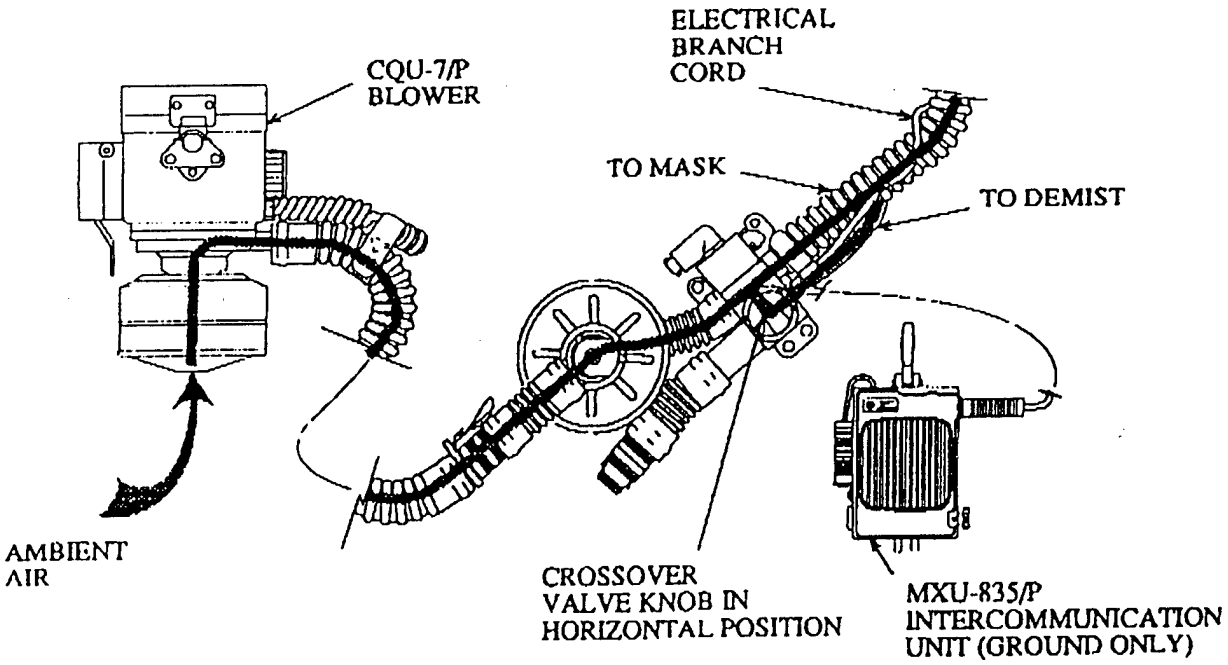

MBU-19/P GROUND OR NON-OXYGEN FLIGHT OPERATING MODE.

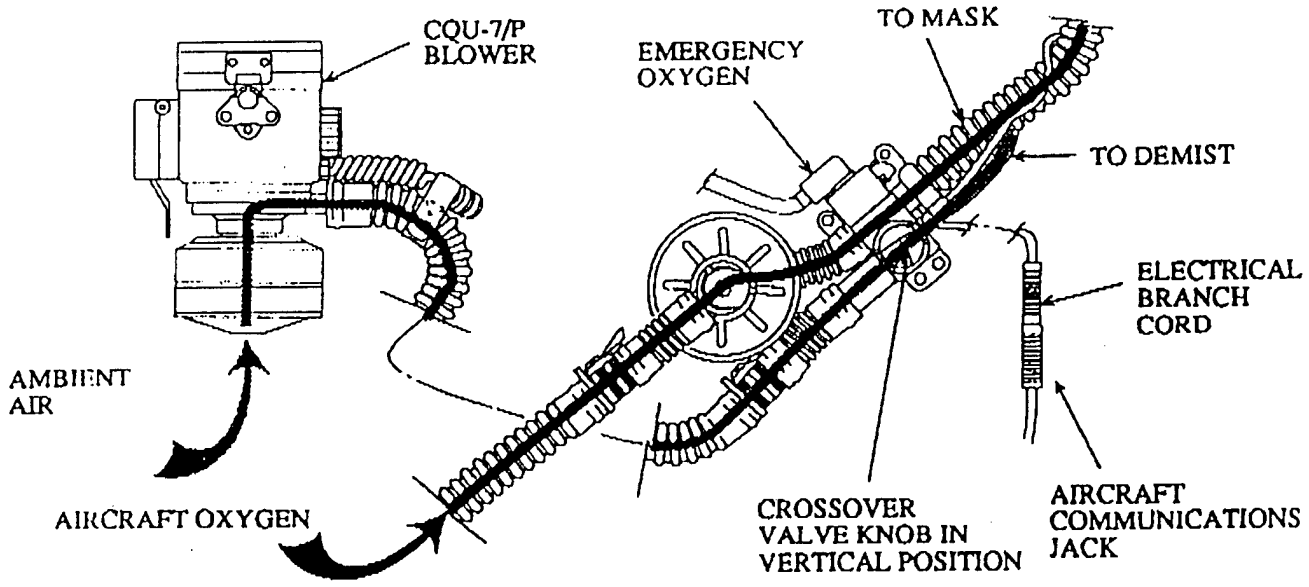

MBU-19/P OXYGEN FLIGHT OPERATING MODE.

Figure 4-2. MBU-19/P Functional Layout.